On the joint network equilibrium of parking and travel choices under mixed traffic of shared and private autonomous vehicles

Zhuoye Zhang[a], Wei Liu[b], Fangni Zhang[a,*]

[a]Department of Industrial and Manufacturing Systems Engineering, University of Hong Kong, Hong Kong, China
[b]Department of Aeronautical and Aviation Engineering, The Hong Kong Polytechnic University, Hong Kong, China

Abstract

This paper investigates the joint network equilibrium of parking and travel route choices in the future mobility paradigm with mixed traffic of private and shared autonomous vehicles. Specifically, we consider that private autonomous vehicle (PAV) travelers need to make both route and parking choices though the vehicle can drive itself to parking after dropping off the traveler. The origin-destination-based shared autonomous vehicle (OD-SAV) ride service allows multiple travelers with a common origin and destination (OD) pair to share the same vehicle, while the routing of OD-SAVs is determined by the operator. In this context, a bi-level model is developed which optimizes the OD-SAV service fare and OD-SAV flow in the upper-level, and specifies the travel demands, route and parking choices, and network traffic equilibrium in the lower-level. In particular, PAV travelers choose their route and parking location to minimize their own travel time or cost, while the routing of OD-SAVs is subject to the decision of the operator. The OD-SAVs controlled by the operator may minimize each vehicle's travel time (user equilibrium, 'UE') or minimize the total travel time of all OD-SAVs operated by the operator (Cournot-Nash equilibrium, 'CN'). The joint equilibrium of travel and parking under either UE or CN routing for OD-SAVs can be modeled as a Variational Inequalities (VI) problem. The uniqueness/non-uniqueness properties of the joint network equilibrium are investigated. Moreover, we examine the OD-SAV service operator's optimal operation decisions subject to the lower-level network equilibrium. Solution approaches are introduced to solve the joint equilibrium and the proposed bi-level model. Numerical studies are conducted to illustrate the model and analytical results, and also to provide further understanding.

Keywords: Shared autonomous vehicles, Private autonomous vehicles, Parking choice, Route choice, Mixed traffic equilibrium, Operation strategies

1. Introduction

Given the rapid development of communication and automation technologies, autonomous vehicles are expected to create new opportunities for realizing smart urban mobility initiatives. Autonomous vehicles may substantially transform people's travel behavior in the future by intelligent motion, adaptive steering control and autonomous parking system (Burns, 2013). In transportation systems, how autonomous vehicles will affect traveler's behavior and potentially change the urban road network traffic patterns and system performance is an important question that should be examined.

In the future autonomous vehicle network, there can be mixed traffic of shared autonomous vehicles and private autonomous vehicles (PAVs), and some travelers may not own a PAV. Origin-destination-based shared autonomous vehicle (OD-SAV) ride service can offer cost-effective and convenient ride-sharing services to travelers with common origin and destination (OD) while PAVs provide better privacy and customization for users. The OD-based mobility service operated with autonomous vehicles was also examined in Narayanan et al. (2022). This study further considers a more general format of OD-SAV service that serves specific direct OD pairs without stopovers, where multiple

*Corresponding author. Email address: fnzhang@hku.hk (F. Zhang)

travelers with a common OD pair can share the same vehicle. Direct OD-based ride service may be favorable with the wide application of autonomous vehicles. This format minimizes the boarding/alighting delays en-route (compared to stop-by-stop services), and reduces the detours due to pickup and dropoff delays at different origins and destinations (compared to door-to-door ride services). It may become a future service paradigm in the era of autonomous vehicles. Moreover, PAVs can drive themselves to park after dropping off the travelers, while taking OD-SAV service travelers do not need to concern parking. This means that PAV or OD-SAV travels relate to different travel and parking considerations, which should be properly quantified in order to assess network traffic patterns with mixed traffic of OD-SAVs and PAVs. This paper fills this gap and extends the literature by investigating the joint network equilibrium of parking and travel route choices under the mixed traffic of OD-SAVs and PAVs.

This paper investigates a future mobility paradigm where travelers can travel with either the PAV or OD-SAV service. On the one hand, traveling with PAV, the traveler needs to make both route and parking choices while the vehicle can drive itself to parking after dropping off the traveler. On the other hand, the OD-SAV ride-sharing service is provided by an operator, which serves specific OD pairs. Multiple travelers with common OD pair can share the same vehicle, and the routing of OD-SAVs is determined by the operator. In this context, we examine how OD-SAVs and PAVs will interact with each other in the network and how their interaction will endogenously affect the network parking and travel patterns and the system efficiency. In particular, the routing of OD-SAVs determined by the operator may follow either user equilibrium (UE) or Cournot-Nash equilibrium (CN) principle (depending on the operation model between users and the operator). Secondly, the complex interactions among PAV trip flow, PAV autonomous parking flow (empty vehicle trip for parking) and OD-SAV traffic flow will be examined, which in turn jointly determine the network traffic equilibrium. This is the first study in the literature to examine such a joint travel and parking equilibrium of PAVs and OD-SAVs. Thirdly, we examine the OD-SAV service operator's optimal operation decisions (trip fare and OD-SAV flow deployment) subject to the joint travel and parking equilibrium, where the operator may either maximize its profit (as a private operator) or maximize the social welfare (as a public operator).

Specifically, this study develops a bi-level model to characterize the joint network equilibrium with respect to PAVs and OD-SAVs (at the lower-level) and to optimize the OD-SAV ride service (at the upper-level). We firstly formulate the lower-level joint travel and parking network equilibrium using the Variational inequality (VI) formulations, where PAVs are considered to follow the UE routing. The routing of OD-SAVs is determined by the operator, who may adopt either the UE or CN principle. Namely, the objective of the OD-SAV routing problem can be the minimization of either each vehicle's travel cost, or the whole OD-SAV fleet's total travel cost. The uniqueness/non-uniqueness properties of the joint network equilibrium are discussed through the VI formulations. Furthermore, in the upper-level model, the optimal trip fare and OD-SAV flow deployment of OD-SAV ride service are examined and compared under profit-maximization and social welfare-maximization. Numerical studies are conducted to generate further insights on the network performance with respect to the parking supplies.

The network equilibrium model developed in this paper benefits from the extensive literature on network traffic assignment model. It has been widely adopted to quantify and analyze network traffic patterns with, for example, single- and multi-class users (Yang & Huang, 2004; Wang et al., 2015; Liu & Wang, 2015; Han et al., 2018), electric vehicles (He et al., 2013, 2014, 2015; Cen et al., 2018; Zhang et al., 2018b), and autonomous vehicles (Chen et al., 2017; Zhang et al., 2019a; Levin et al., 2020; Xie & Liu, 2022; Kang et al., 2022). The system equilibrium where travelers follow Wardrop (1952)'s first and second principles are characterized as the UE and system optimum (SO), respectively. Under certain circumstances, some travelers may seek to minimize their total travel cost as a group, instead of individual cost. Such behavior is often modeled as the CN equilibrium (Harker, 1988; Yang et al., 2007). A typical example is that a truck company may minimize the total travel cost by optimally routing its own vehicles. Recently, Zhang et al. (2019a,b) investigated autonomous vehicles' travel and parking patterns under homogeneous autonomous vehicle traffic environments, and they found that empty vehicle trips looking for parking account for a significant amount of road traffic and should be properly managed.

Although no study has systematically investigated the joint travel and parking network equilibrium of mixed traffic of private and shared autonomous vehicles, the literature has examined the shared automated mobility service design and management and autonomous vehicle parking problems in a few different aspects (e.g., Su & Wang, 2020; Tang et al., 2021; Chen & Liu, 2022; Guo et al., 2022). Different formats of shared autonomous vehicle services have been studied in the existing studies (e.g., Stocker & Shaheen, 2018; Narayanan et al., 2020; Golbabaei et al., 2021). One format is similar to the ride-sourcing service in the dial-a-ride fashion (e.g., Fagnant & Kockelman, 2018; Gurumurthy & Kockelman, 2018), where travelers can either ride alone or share the vehicle with travelers of different OD pairs.

Another format of service is similar to the public transport and ride-pooling services (Ke et al., 2020; Zhang & Zhang, 2022), which serves specific OD pairs. However, with autonomous driving, the route of shared autonomous vehicles can be more flexible than the fixed-route services provided by traditional public transport (e.g., Ainsalu et al., 2018). This study focuses on the latter service format, i.e., similar to OD-based public transport services with autonomous driving. Some studies examined the cooperation between the shared mobility service and public transit. For example, Shen et al. (2018) integrated shared autonomous vehicle with the public transport as a first-mile solution, where the public transit service quality can be further improved. Pinto et al. (2020) developed a bi-level model to design the transit network taking into account shared autonomous vehicles. Their results indicated that user experience can be improved without increasing the transit budget. For a detailed review of shared autonomous vehicle mobility services, one may refer to Golbabaei et al. (2021).

Existing studies of autonomous vehicle parking problems mainly focused on the self-parking capability of PAVs and the optimal parking supply (Liu, 2018; Zhang et al., 2019b; Levin et al., 2020; Zhang et al., 2021; Bahk et al., 2022; Mondal et al., 2022). The autonomous vehicle parking problem has not been jointly considered with the shared autonomous vehicle ride service, where there exist complex cross-modal flow interactions, travel flow and parking flow interactions, and different vehicle routing behaviors in the context of mixed traffic of private and shared autonomous vehicles. Regarding the human-driven vehicle parking problem, the cruising for parking (Liu & Geroliminis, 2016; Gu et al., 2020), parking reservation (Yang et al., 2013; Shao et al., 2016; Chen et al., 2019; Levin & Boyles, 2020), parking pricing (Zhang et al., 2005, 2008; Wu et al., 2021) and parking sharing (Zhang et al., 2020; Jian et al., 2020; Liu et al., 2021) have been studied in the literature.

The rest of the paper is organized as follows. Section 2 presents the model description and formulates the travel costs with respect to OD-SAVs and PAVs. In Section 3, the lower-level joint network equilibrium considering the parking choice and travel route choice is formulated, and the solution algorithms to the lower-level problem are presented. Section 4 examines the optimal operation decisions of the OD-SAV service operator and presents the solution algorithms to the bi-level problem. Section 5 presents the numerical results to illustrate the model and findings. Finally, conclusions, limitations and future research directions are discussed in Section 6.

2. Problem description

We consider a road network denoted by $G(N, E)$, where N represents the set of nodes and E denotes the set of links. For each link $e \in E$, the link travel time function, $t_e(x_e)$, is assumed to be convex, non-negative, differentiable, and monotonically increasing with respect to the link traffic flow x_e. An OD pair is denoted by (r, s) that belongs to the OD pair set M, where $r \in R$ is the origin node and $s \in S$ is the destination node (note that the origin set R and the destination set S are both subsets of N). The parking node is denoted by p, where $p \in P$ and P represents the parking node set and P is a subset of N. The route set between origin r and destination s is represented by W_{rs}. A list of main notations is provided in the Appendix A.

We consider that the demands for PAV and OD-SAV rides are both elastic, which decrease with the travel costs for PAV and OD-SAV, respectively.[1] The PAV trip and OD-SAV trip are as follows. The PAV will first drive a traveler to his or her destination, and then look for and drive itself to a vacant parking space (can be at a location different from the destination of the traveler). The trip of PAVs consists of two parts: the first part is from the traveler's origin to the traveler's destination, and the second part is from the traveler's destination to the selected parking location. The parking location choice should minimize the PAV traveler's travel cost, and the routing of PAVs should minimize the travel time. For the OD-SAVs, we consider that there are ride services between each OD pair (e.g., between residential areas and the central business district) and travelers have to share the OD-SAV with others, where trip fares and OD-SAV flow for each OD pair are decision variables of the OD-SAV service operator.[2]

[1] The PAV and OD-SAV demands represent the aggregate PAV and OD-SAV trip volumes in the long-term equilibrium, respectively. The elastic demand functions implicitly accommodate the mode shift behavior, which represents the aggregation of travel choices of all travelers. For a specific individual, his/her travel mode may vary, e.g., he/she may travel with PAV on one day (contribute to the equilibrium PAV demand), and on another day, he/she may travel with OD-SAV service (contribute to the equilibrium OD-SAV demand) or other alternatives.

[2] As a clarification of the terms, OD-SAV demand represents the travel demand for the OD-SAV service for each OD pair, where the unit is persons per unit time. The OD-SAV flow represents the vehicle flow of OD-SAV service between each OD pair, or the service frequency, where the unit is services per unit time.

As discussed earlier, the routing of OD-SAVs is determined by the operator, who may adopt either the UE or CN principle, while PAVs always follow the UE routing. When OD-SAVs follow the UE routing, the joint travel and parking equilibrium is referred to as the "joint user equilibrium". When OD-SAVs follow the CN routing, the joint travel and parking equilibrium is referred to as the "joint mixed equilibrium", i.e., routing of PAVs and OD-SAVs follows different principles. This is similar to the mixed equilibrium considered in existing studies, e.g., Yang et al. (2007). However, existing mixed equilibrium studies did not consider joint equilibrium of travel and parking and mixed traffic of PAVs and OD-SAVs.

The bi-level problem considered in this paper is depicted in Fig. 1. In the upper-level, the OD-SAV operator optimizes the trip fare and OD-SAV flow for either profit-maximization or social welfare-maximization. The lower-level problem concerns the "joint user equilibrium" (Scenario 1) or the "joint mixed equilibrium" (Scenario 2) as described above.

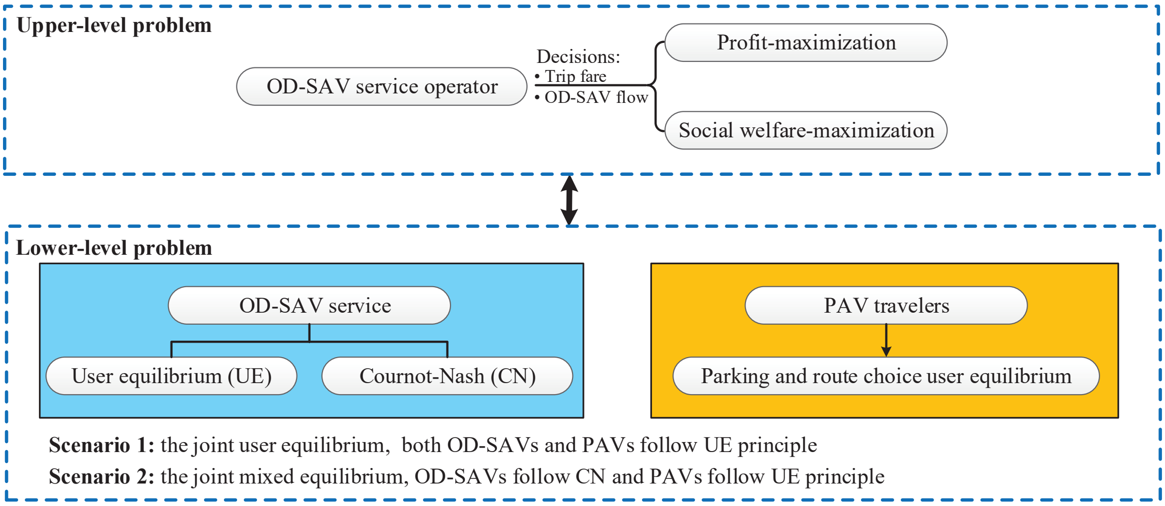

Fig. 1. The overall framework of the bi-level models in this paper

2.1. *Private autonomous vehicles*

We now introduce the travel and parking for the PAV travelers and then formulate the PAV travel cost. The PAV travelers will choose a parking location $p \in P$ to minimize the total travel cost from origin $r \in R$ to the parking location $p \in P$ via the destination $s \in S$. Between a traveler's origin r and destination s ($r \rightarrow s$), the PAV traveler will choose the shortest route to minimize the travel time, respectively. Similarly, the PAV traveler will choose the shortest route between the traveler's destination s and parking location p (i.e., $s \rightarrow p$), which is a self-driving process to parking.

The travel cost $c^a_{rs,p}$ for PAVs (superscript 'a' indicates the PAV mode) that depart from origin r, drop off travelers at destination s, and then arrive at the parking location p by self-driving can be expressed as follows:

$$c^a_{rs,p} = \beta t_{rs} + \alpha t_{sp} + Z_p + \sigma + \lambda_p, \quad \forall (r, s) \in M, p \in P. \tag{1}$$

The first term βt_{rs} and second term αt_{sp} represent the travel time costs, where t_{rs} is the travel time between origin r and destination s, t_{sp} is the travel time between destination s and parking location p. The travel time is subject to the equilibrium route choice and network traffic condition. β is the unit time travel cost for the OD travel trip, which includes the value of time of travelers, fuel and energy consumption, etc. α represents the unit time cost for parking trip with no traveler onboard, which is expected to be less costly than OD travel, i.e., $\alpha < \beta$. The third term Z_p and the fourth term σ represent the parking fee at parking location p and the vehicle ownership cost (the cost in relation to vehicle acquisition that is converted into a cost per trip). The last term λ_p is the advance booking cost for parking (e.g., inconvenience due to booking early in order to secure a parking space or the opportunity cost), which is associated with competition for parking and parking capacity constraints, i.e., $d_p \leq C_p, \forall p \in P$, where d_p and C_p represent the parking demand and parking capacity at parking location $p \in P$. The advance booking cost is defined by the following:

$$\lambda_p(C_p - d_p) = 0; \lambda_p \geq 0; C_p - d_p \geq 0, \quad \forall p \in P. \tag{2}$$

The above advance booking cost for parking is similar to that for the high-speed railway system and parking-sharing discussed in Xu et al. (2018) and Liu et al. (2021). The advance booking cost is the shadow price of the parking capacity constraint and endogenously determined by the parking demand and capacity. In particular, when $d_p < C_p$, i.e., demand is less than supply at destination $s \in S$, there is no need to book in advance and $\lambda_p = 0$; when $d_p = C_p$, the advance booking cost λ_p can be positive since PAV travelers have to compete with each other in order to secure a parking space.

The PAV demand is a non-negative and strictly decreasing function with respect to the equilibrium travel cost c^a_{rs} for each OD pair (r, s), which is given by:

$$q^a_{rs} = f^a_{rs}\left(c^a_{rs}\right), \quad \forall (r, s) \in M, \tag{3}$$

where q^a_{rs} denotes the PAV travel demand between OD pair (r, s), and $f^a_{rs}(\cdot)$ is a non-negative and strictly decreasing function for OD pair (r, s), i.e., $f^{a,'}_{rs} = df^a_{rs}/dc^a_{rs} < 0$.

2.2. Shared-autonomous vehicle ride service

The travel cost by OD-SAV service includes the following four parts: the trip fare, the travel time cost associated with in-vehicle time, waiting time, and the inconvenience cost due to sharing the same vehicle with other travelers. The generalized travel cost of OD-SAV ride service (OD-SAV mode indicated by the superscript 'b') can be expressed as follows:

$$c^b_{rs} = F_{rs} + \beta\left(t_{rs} + \phi\left(y_{rs}, q^b_{rs}\right)\right) + \delta_{rs}, \quad \forall (r, s) \in M. \tag{4}$$

The first term F_{rs} represents the trip fare per traveler per trip for OD pair (r, s). The second term $\beta\left(t_{rs} + \phi\left(y_{rs}, q^b_{rs}\right)\right)$ denotes the time cost, where β is the value of time, t_{rs} is the in-vehicle travel time from the origin node r to the destination node s, and $\phi\left(y_{rs}, q^b_{rs}\right)$ is the service waiting time, which is a non-negative and differentiable function of the OD-SAV flow y_{rs} and the demand of OD-SAV ride service q^b_{rs}. In particular, y_{rs} is the OD-SAV flow between OD pair (r, s) (corresponding to a certain fleet size) and q^b_{rs} is the demand volume of OD-SAV ride service between OD pair (r, s). The waiting time $\phi(\cdot)$ strictly decreases with OD-SAV flow y_{rs} and increases with demand q^b_{rs}, i.e., $\phi'_{y_{rs}} = \partial\phi/\partial y_{rs} < 0$ and $\phi'_{q^b_{rs}} = \partial\phi/\partial q^b_{rs} > 0$. The average waiting time is adopted to measure the crowding effect of travelers, and we do not consider the hard vehicle capacity constraint. The third term in Eq. (4), δ_{rs}, represents a constant inconvenience cost for travelers due to sharing the vehicle with others between OD pair (r, s).

When the OD-SAVs follow the UE routing, all OD-SAV travelers of the same OD pair will experience minimal and identical travel cost. When the routing of OD-SAVs follows the CN principle, OD-SAV travelers between the same OD pair may take different routes. We consider that the OD-SAV service demand q^b_{rs} for each OD pair (r, s) is a decreasing function of the average cost $\overline{c}^b_{rs}$ (average over all OD-SAV travelers between the same OD pair). For both the UE routing and CN routing, the travel demand q^b_{rs} for the OD-SAV ride service can be given as follows:

$$q^b_{rs} = f^b_{rs}\left(\overline{c}^b_{rs}\right), \quad \forall (r, s) \in M, \tag{5a}$$

$$\overline{c}^b_{rs} = \frac{\sum_{W_{rs}} c^b_{rs,w} v^b_{rs,w}}{\sum_{W_{rs}} v^b_{rs,w}}, \quad \forall (r, s) \in M, \tag{5b}$$

where $f^b_{rs}(\cdot)$ is a non-negative and strictly decreasing function for OD pair (r, s), i.e., $f^{b,'}_{rs} = df^b_{rs}/d\overline{c}^b_{rs} < 0$. $\overline{c}^b_{rs}$ is the average cost of OD-SAV travelers for OD pair (r, s). This term will be used to represent the equilibrium travel cost for OD-SAV travelers following the UE or CN routing principle, respectively. $c^b_{rs,w}$ and $v^b_{rs,w}$ represent the travel cost and OD-SAV flow of route w between OD pair (r, s), respectively.

3. Lower-level problem: joint equilibrium of parking location choice and route choice

We now formulate the joint network equilibrium considering elastic travel demand, parking location choice and route choice. PAV travelers minimize their individual travel cost when choosing parking (self-driving between the destination and the parking location), and minimize their travel time when choosing the route (traveling between the OD pair), which follows the "UE routing". For OD-SAV ride service, we consider two scenarios: (i) OD-SAVs follow UE routing; (ii) OD-SAVs follow CN routing. Given the OD-SAV ride service operation strategies in the upper-level problem (as described in Fig. 1), i.e., trip fare F_{rs} and OD-SAV flow y_{rs}, we formulate the "joint user equilibrium" (both OD-SAVs and PAVs follow the UE routing) and "joint mixed equilibrium" (PAVs follow the UE routing and OD-SAVs follow the CN routing) in Section 3.1.1 and Section 3.2.1, respectively. We develop VI formulations that facilitate the discussion of the uniqueness/non-uniqueness properties of the network equilibrium in Section 3.1.2 and Section 3.2.2. Solution procedures to solve the above network equilibrium are introduced in Section 3.1.3 and Section 3.2.3.

3.1. Joint user equilibrium with PAVs and OD-SAVs

In this subsection, the joint user equilibrium with respect to PAVs and OD-SAVs is formulated in Section 3.1.1, where both OD-SAVs and PAVs follow Wardrop's first principle (UE). Then, the equivalent VI formulation is developed in Section 3.1.2 and the solution procedure is presented in Section 3.1.3.

3.1.1. Joint user equilibrium formulation

(Parking trip integrated PAV demand) A PAV trip involves two parts: from origin to destination and from destination to parking. To ease and facilitate the model formulation and presentation, we define a parking trip integrated demand by combining the demand from origin to destination and demand from destination to parking. Specifically, the parking trip integrated PAV demand between an origin r and a destination s, Q^a_{rs}, is given by

$$Q^a_{rs} = q^a_{rs} + \overline{q}^a_{rs}, \tag{6}$$

where q^a_{rs} is the demand from origin r to destination s, i.e., $(r, s) \in M$ and $\overline{q}^a_{rs}$ is the demand from destination $r \in S$ to parking $s \in P$. Note that $q^a_{rs} = 0$ or $\overline{q}^a_{rs} = 0$ if such demand does not exist. Furthermore, we let M' denote the parking trip integrated OD set, which is an integration of the OD set for trips between travelers' origins and destinations and the OD set for trips between travelers' destination and parking location.

(Flow conservation, path travel time, and non-negativity) We now introduce the parking flow conservation in Eq. (7), route and link flow conservation and route travel time in Eq. (8) and non-negativity constraints in Eq. (9).

$$\textbf{Parking flow conservation:} \begin{cases} q^a_{rs} = \sum_p q^a_{rs,p}, \forall (r,s) \in M, & \text{(7a)} \\ q^a_{s,p} = \sum_r q^a_{rs,p}, \forall s \in S, p \in P, & \text{(7b)} \\ \sum_r q^a_{rs} = \sum_p q^a_{s,p}, \forall s \in S, & \text{(7c)} \\ \sum_{(r,s)\in M} q^a_{rs} = \sum_s \sum_p q^a_{s,p}, & \text{(7d)} \\ \sum_{(r,s)\in M} q^a_{rs,p} \le C_p, \forall p \in P, & \text{(7e)} \end{cases}$$

$$
\textbf{Route/link flow conservation and route time:}\begin{cases}
Q^a_{rs} - \sum\limits_{w\in W_{rs}} v^a_{rs,w} = 0, \forall (r,s) \in M', & \text{(8a)}\\
x^a_e = \sum\limits_{(r,s)\in M'} \sum\limits_{w\in W_{rs}} v^a_{rs,w}\cdot \delta^{rs}_{e,w}, \forall e\in E, & \text{(8b)}\\
y_{rs} - \sum\limits_{w\in W_{rs}} v^b_{rs,w} = 0, \forall (r,s)\in M, & \text{(8c)}\\
x^b_e = \sum\limits_{(r,s)\in M} \sum\limits_{w\in W_{rs}} v^b_{rs,w}\cdot \delta^{rs}_{e,w}, \forall e\in E, & \text{(8d)}\\
x_e = x^a_e + x^b_e, \forall e\in E, & \text{(8e)}\\
t_{rs,w} = \sum\limits_{e\in E} t_e(x_e)\cdot \delta^{rs}_{a,w}, \forall (r,s)\in M', w\in W_{rs}, & \text{(8f)}
\end{cases}
$$

$$
\textbf{Non-negativity constraints:}\begin{cases}
q^a_{rs}, q^a_{rs,p} \geq 0, \forall (r,s)\in M, & \text{(9a)}\\
v^a_{rs,w}, v^b_{rs,w} \geq 0, \forall (r,s)\in M', w\in W_{rs}, & \text{(9b)}\\
x^a_e, x^b_e \geq 0, \forall e \in E. & \text{(9c)}
\end{cases}
$$

In the above, $v^a_{rs,w}$ and $v^b_{rs,w}$ represent the PAV and OD-SAV flows on route w from OD pair (r, s), respectively. x^a_e and x^b_e denote the link flows for PAVs and OD-SAVs, respectively. $\delta^{rs}_{e,w}$ is the link-route incidence index, which equals one if link e is part of route w connecting OD pair (r, s), and zero otherwise. $t_{rs,w}$ represents the travel time of route $w \in W_{rs}$.

Eq. (7a) says that, for each OD pair (r, s), the PAV demand q^a_{rs} should equal the parking flows to different parking locations. Eq. (7b) says that the parking flow $q^a_{s,p}$ from destination s to the parking location p should equal the sum of parking flows from different origins. Eq. (7c) states that at each destination node $s \in S$, the total inflow $\sum_r q^a_{rs}$ should equal the total outflow $\sum_p q^a_{s,p}$. Eq. (7d) says that the total flow over different OD pairs should equal the total parking flow. Eq. (7e) is the location-specific parking capacity constraint.

Eq. (8a) says that for PAVs, the parking trip integrated OD flow is equal to the summation of route flows for each OD pair. Eq. (8c) states that the sum of OD-SAV route flows between OD pair (r, s) is equal to the total OD-SAV flow y_{rs} that is set by the OD-SAV operator. Eq. (8b) and Eq. (8d) describe the relationship between link flow and route flow for PAVs and OD-SAVs, respectively, where $\delta^{rs}_{e,w}$ is the link-route incidence index. Eq. (8e) states that the total link flow x_e equals the sum of PAV link flow x^a_e and OD-SAV link flow x^b_e for each link $e \in E$. Eq. (8f) defines the route travel time as a summation of link travel times.

Eq. (9) contains the non-negativity constraints with respect to demand, route flow, and link flow for both PAVs and OD-SAVs.

Let Φ denote the feasible set for PAV demand $\boldsymbol{q^a} = \{q^a_{rs}\}$, parking choice $\boldsymbol{q_p} = \left\{q^a_{rs,p}\right\}$, and link flow pattern $\boldsymbol{x^a} = \{x^a_e\}$ and $\boldsymbol{x^b} = \left\{x^b_e\right\}$ that are subject to the constraints in Eqs. (7)-(9).

(Elastic demand equilibrium) We now introduce the elastic demand equilibrium for PAV mode, which, following Sheffi (1985), can be formulated as follows:

$$
\left(c^a_{rs} - f^{a,-1}_{rs}\left(q^a_{rs}\right)\right) q^a_{rs} = 0, \quad \forall (r,s)\in M, \tag{10a}
$$

$$
c^a_{rs} - f^{a,-1}_{rs}\left(q^a_{rs}\right) \geq 0, \quad \forall (r,s)\in M, \tag{10b}
$$

$$
q^a_{rs} \geq 0, \quad \forall (r,s)\in M, \tag{10c}
$$

where c^a_{rs} denotes the equilibrium travel cost for trips between OD pair (r, s), and $f^{a,-1}_{rs}(\cdot)$ is the inverse demand function associated with the PAV mode. Similarly, the elastic demand equilibrium for OD-SAV mode can be expressed as follows:

$$
\left(\overline{c}^b_{rs} - f^{b,-1}_{rs}\left(q^b_{rs}\right)\right) q^b_{rs} = 0, \quad \forall (r,s)\in M, \tag{11a}
$$

$$
\overline{c}^b_{rs} - f^{b,-1}_{rs}\left(q^b_{rs}\right) \geq 0, \quad \forall (r,s)\in M, \tag{11b}
$$

$$
q^b_{rs} \geq 0, \quad \forall (r,s)\in M, \tag{11c}
$$

where $\overline{c}^b_{rs}$ denotes the average cost for trips between OD pair (r, s) (equal to the equilibrium cost when OD-SAVs follow the UE routing), and $f^{b,-1}_{rs}(\cdot)$ is the inverse demand function associated with the OD-SAV mode.

(PAV parking location choice equilibrium) Based on the generalized travel cost of PAV travelers defined in Eq. (1), the PAVs' parking choice equilibrium conditions can be expressed as follows:

$$\left(c^a_{rs,p} - c^a_{rs}\right) q^a_{rs,p} = 0, \ \ \forall (r, s) \in M, p \in P, \tag{12a}$$

$$c^a_{rs,p} - c^a_{rs} \geq 0, \ \ \forall (r, s) \in M, p \in P, \tag{12b}$$

$$q^a_{rs,p} \geq 0, \ \ \forall (r, s) \in M, p \in P, \tag{12c}$$

where $c^a_{rs,p}$ represents the travel cost of PAV travelers from origin r to destination s with a parking location p, $c^a_{rs} = min\left\{c^a_{rs,p}\right\}$ denotes the equilibrium travel cost for trips between OD pair (r, s), $q^a_{rs,p}$ is parking demand at parking location p of OD pair (r, s).

(UE routing for PAVs and OD-SAVs) The route choice equilibrium conditions for PAVs and OD-SAVs can be written as:

$$(t_{rs,w} - t_{rs})v_{rs,w} = 0, w \in W_{rs}, (r, s) \in M', \tag{13a}$$

$$t_{rs,w} - t_{rs} \geq 0, w \in W_{rs}, (r, s) \in M', \tag{13b}$$

$$v_{rs,w} \geq 0, w \in W_{rs}, (r, s) \in M', \tag{13c}$$

where $t_{rs,w}$ and t_{rs} represent the travel time of route $w \in W_{rs}$ and the minimal travel time from r to s, respectively, and $t_{rs} = min\left\{t_{rs,w}, w \in W_{rs}\right\}$. Note that the above routing conditions are for both PAVs and OD-SAVs.

Eq. (10), Eq. (11), Eq. (12) and Eq. (13) provide the joint user equilibrium conditions in relation to the elastic demands for PAV and OD-SAV, PAV parking choice, and PAV and OD-SAV route choice.

3.1.2. VI formulations and properties of the joint user equilibrium

In this subsection, we develop the VI (Smith, 1979; Dafermos, 1980) formulation for the joint user equilibrium. Regarding the PAV demand $\boldsymbol{q^a} = \{q^a_{rs}\}$, OD-SAV demand $\boldsymbol{q^b} = \left\{q^b_{rs}\right\}$, PAV parking choice $\boldsymbol{q_p} = \left\{q^a_{rs,p}\right\}$ and link flow pattern $\boldsymbol{x^a} = \{x^a_e\}$ and $\boldsymbol{x^b} = \left\{x^b_e\right\}$ at the joint user equilibrium, we have the following results.

Proposition 3.1. *The PAV demand, OD-SAV demand, PAV parking choice, and link flow pattern* $\left(\boldsymbol{q^{a,*}}, \boldsymbol{q^{b,*}}, \boldsymbol{q^*_p}, \boldsymbol{x^{a,*}}, \boldsymbol{x^{b,*}}\right)$ *reaches the joint user equilibrium defined in Eqs. (10)-(13) if and only if it solves the following VI problem:*

$$\sum_{(r,s)\in M} \sum_{p} c^{a,*}_{rs,p}(q^a_{rs,p} - q^{a,*}_{rs,p}) - \sum_{(r,s)\in M} f^{a,-1}_{rs}(q^{a,*}_{rs})(q^a_{rs} - q^{a,*}_{rs}) + \sum_{e\in E} t_e(x^*_e)(x^a_e - x^{a,*}_e)$$
$$- \sum_{(r,s)\in M} f^{b,-1}_{rs}\left(q^{b,*}_{rs}\right)\left(q^b_{rs} - q^{b,*}_{rs}\right) + \sum_{e\in E} t_e(x^*_e)\left(x^b_e - x^{b,*}_e\right) \geq 0, \tag{14}$$

subject to $(\boldsymbol{q^a}, \boldsymbol{q^b}, \boldsymbol{q_p}, \boldsymbol{x^a}, \boldsymbol{x^b}) \in \Phi$.

Proof. See Appendix B. □

Proposition 3.1 establishes the equivalency between the joint user equilibrium defined in Eqs. (10)-(13) and the VI problem defined in Eq. (14). A solution to the proposed VI problem in Eq. (14) exists since all the functions and terms in Eq. (14) are continuous and the set of feasible solutions is non-empty and compact (Facchinei & Pang, 2007; Liu et al., 2021).

Let $d_p = \sum_{(r,s)\in M} q^a_{rs,p}, \forall p \in P$ or $\boldsymbol{d} = \left\{d_p\right\}$ denote the total parking demand at parking location $p \in P$. We are now ready to discuss the uniqueness/non-uniqueness with respect to the PAV demand pattern $\boldsymbol{q^a} = \{q^a_{rs}\}$, OD-SAV demand pattern $\boldsymbol{q^b} = \left\{q^b_{rs}\right\}$, PAV travelers' parking choice pattern $\boldsymbol{q_p} = \left\{q^a_{rs,p}\right\}$, the link flow pattern $\boldsymbol{x} = \{x_e\}$ and location-specific parking flow pattern $\boldsymbol{d} = \left\{d_p\right\}$ (or parking occupancy rate $u_p = d_p/C_p$ at each parking lot).

Proposition 3.2. *Under given PAV demand pattern and parking choice pattern* $\left(\boldsymbol{q^a}, \boldsymbol{q_p}\right)$*, the link flow pattern* $\boldsymbol{x^*}$ *and OD-SAV demand pattern* $\boldsymbol{q^{b,*}}$ *at the joint user equilibrium must be unique.*

Proof. When the PAV demand pattern $\boldsymbol{q^a}$ and parking choice $\boldsymbol{q_p}$ are given, the parking trip integrated demand pattern $Q^a_{rs}, \forall (r, s) \in M'$ can be uniquely determined. Moreover, the OD-SAV flow $\{y_{rs}\}$ is also given. The original joint user equilibrium problem reduces to a standard deterministic traffic assignment problem with given demand (Sheffi, 1985). Since the link travel time is a strictly increasing function of the link flow, there will be a unique link flow pattern $\boldsymbol{x}^*$ (Patriksson, 2015). Since $\boldsymbol{x}^*$ is unique, the OD-specific travel cost of OD-SAV travelers can be determined accordingly, which correspond to a unique OD-SAV demand pattern $\boldsymbol{q^b} = \left\{q^b_{rs}\right\}$ based on Eq. (5). □

Proposition 3.3. *Given the equilibrium PAV demand pattern* $\boldsymbol{q^{a,*}}$*, when we have different parking choice patterns* $\boldsymbol{q'_p}$ *and* $\boldsymbol{q''_p}$*, the link flow pattern* $\boldsymbol{x}^*$ *and OD-SAV demand pattern* $\boldsymbol{q^{b,*}}$ *at the joint user equilibrium must be unique.*

Proof. See Appendix C. □

Proposition 3.4. *The PAV demand pattern* $\boldsymbol{q^{a,*}}$ *at the joint user equilibrium is unique.*

Proof. See Appendix D. □

Proposition 3.5. *At the joint user equilibrium, the PAV demand pattern* $\boldsymbol{q^{a,*}}$*, link flow pattern* $\boldsymbol{x}^*$*, and OD-SAV demand pattern* $\boldsymbol{q^{b,*}}$ *can be uniquely determined.*

Proposition 3.5 is immediate from Proposition 3.2-3.4. However, the equilibrium parking choice pattern $\boldsymbol{q^*_p}$ may not be unique. This is consistent with the finding of Zhang et al. (2019a), where the non-uniqueness of the parking choice pattern has been illustrated with a small network example. While $\boldsymbol{q^*_p}$ may not be unique, the total parking flow at each parking location is unique, which is stated below.

Proposition 3.6. *The total parking flow* d_p *and parking occupancy rate* $\mu_p = d_p/C_p, \forall p \in P$*, at each parking location* p *at the joint user equilibrium must be unique.*

Proof. From Proposition 3.5, we know that the link flow pattern $\boldsymbol{x}$ at the joint user equilibrium is unique. The total parking flow d_p can be calculated as the summation of all incoming link flows minus all outflows at each parking location $p \in P$, and thus is unique. It follows that the parking occupancy rate u_p at each parking location can be uniquely determined. □

Proposition 3.6 states that though parking choice pattern $\boldsymbol{q^*_p}$ may not be unique at the joint user equilibrium, the total parking demand and parking occupancy rate at any parking location can be uniquely determined. This means that the location-specific parking conditions can be consistently assessed while users of particular parking locations may vary.

3.1.3. Solution procedure for the joint user equilibrium

The joint user equilibrium involves elastic demand, the PAV parking choice and the route choice for both OD-SAVs and PAVs. The general idea to solve the joint user equilibrium problem is as follows. Firstly, given the PAV demand vector $\boldsymbol{q^a} = \{q^a_{rs}\}$, we first assign the parking flow (parking choice), i.e., $\boldsymbol{q_p} = \left\{q^a_{rs,p}\right\}$. Based on the PAV demand, parking demand, OD-SAV flow (OD-specific), we can obtain the combined network demand (consists of both PAVs and OD-SAVs) $\boldsymbol{q} = \{q_{rs}\}$. Then, the link flow pattern can be obtained by solving the deterministic traffic assignment via the Frank-wolf method (or similar convex combination methods). Secondly, based on the obtained link flow pattern and resulting costs, we can re-calculate the PAV demand and parking choice. The above procedure is repeated until a certain convergence criterion is met. The solution procedure to solve the joint user equilibrium is described in Algorithm 1.

In Algorithm 1, we need to use the all-or-nothing method to assign the PAV demand to different parking locations in Step 1(*ii*) and Step 3(*ii*) to obtain the parking choice, i.e., $\boldsymbol{q_{p,(0)}}$ and $\boldsymbol{m_{p,(n+1)}}$, subject to the parking capacity constraints, which is to solve the following optimization problem:

$$\underset{\boldsymbol{m_{p,(n+1)}}}{Min} \sum_{(r,s)\in M} \sum_{p} c^a_{rs,p,(n+1)} \cdot m_{rs,p,(n+1)}, \tag{17}$$

Algorithm 1 Solution procedure for the joint user equilibrium

1: Initialization

(i) Set iteration number $n = 0$, traffic flow pattern $\boldsymbol{x_{(0)}} = 0$ and initialize PAV demand pattern $\boldsymbol{q^a_{(0)}}$;

(ii) Calculate the travel cost of PAV travelers denoted by $c^a_{rs,p,(0)}$ according to the free flow traffic pattern $\boldsymbol{x_{(0)}} = 0$, and then calculate the parking choice $\boldsymbol{q_{p,(0)}}$ (based on the PAV demand $\boldsymbol{q^a_{(0)}}$) according minimal travel cost parking subject to parking capacity constraints.

2: Traffic assignment

(i) Calculate the parking trip integrated PAV travel demand $\boldsymbol{Q_{(n)}} = \left\{Q^a_{rs,(n)}\right\}$ according to Eq. (6);

(ii) Solve the user equilibrium traffic flow pattern $\boldsymbol{x_{(n+1)}}$ by the Frank-Wolfe algorithm given the parking trip integrated PAV demand $\left\{Q^a_{rs,(n)}\right\}$ and OD-SAV flow $\{y_{rs}\}$.

The convergence criterion for the Frank-Wolfe algorithm: We define the following discrepancy term

$$\eta_{u,x} = \frac{\sqrt{\sum\limits_{e\in E}\left(x_{e,(j+1)} - x_{e,(j)}\right)^2}}{\sum\limits_{e\in E} x_{e,(j)}}, \tag{15}$$

where j denotes the traffic assignment iteration number. Let ϵ_x represent a sufficiently small convergence threshold. If $\eta_{u,x} \leq \epsilon_x$, the Frank-Wolfe algorithm stops.

3: Updating the parking choice and PAV travel cost

(i) Update the travel cost of PAV mode $c^a_{rs,p,(n+1)}$ according to the link flow pattern $\boldsymbol{x_{(n+1)}}$, and then calculate the PAV demand $\boldsymbol{k^a_{(n+1)}} = \left\{f^a_{rs}\left(c^a_{rs,(n+1)}\right)\right\}$ based on the minimal route cost $c^a_{rs,(n+1)} = min\left\{c^a_{rs,p,(n+1)}\right\}$;

(ii) Obtain the parking choice $\boldsymbol{m_{p,(n+1)}}$ by assigning the PAV demand $\boldsymbol{k^a_{(n+1)}}$ to the parking location using all-or-nothing method on the basis of the minimal travel cost $c^a_{rs,(n+1)}$;

(iii) Update the PAV demand and parking choice by using the method of successive average (MSA): $\boldsymbol{q^a_{(n+1)}} = \frac{n}{n+1}\boldsymbol{q^a_{(n)}} + \frac{1}{n+1}\boldsymbol{k^a_{(n+1)}}$, $\boldsymbol{q_{p,(n+1)}} = \frac{n}{n+1}\boldsymbol{q_{p,(n)}} + \frac{1}{n+1}\boldsymbol{m_{p,(n+1)}}$.

4: Convergence criterion

The total relative gap on each vector for iteration n is calculated as follows:

$$\eta_{u,p} = \frac{\sqrt{\sum\limits_{(r,s)\in M}\left(q^a_{rs,(n+1)} - q^a_{rs,(n)}\right)^2}}{\sum\limits_{(r,s)\in M} q^a_{rs,(n)}} + \frac{\sqrt{\sum\limits_{(r,s)\in M}\sum\limits_{p}\left(q^a_{rs,p,(n+1)} - q^a_{rs,p,(n)}\right)^2}}{\sum\limits_{(r,s)\in M}\sum\limits_{p} q^a_{rs,p,(n)}}. \tag{16}$$

If $\eta_{u,p} \leq \epsilon_p$, where ϵ_p represents a sufficiently small constant, the algorithm terminates and we can calculate the OD-SAV demand $\boldsymbol{q^b} = \left\{q^b_{rs}\right\}$ based on the link flow pattern, otherwise $n = n + 1$ and go to Step 2.

---

subject to:

$$\sum_{(r,s)\in M} m_{rs,p,(n+1)} \leq C_p, \tag{18a}$$

$$\sum_{p} m_{rs,p,(n+1)} = k^a_{rs,(n+1)}, \forall\,(r,s) \in M. \tag{18b}$$

Given the PAV travel cost $c^a_{rs,p,(n+1)}$ and PAV demand $k^a_{rs,(n+1)}$, the above problem is a linear programming that can be readily solved by the simplex method or other more advanced linear programming solution techniques.

3.2. The joint mixed equilibrium with PAVs and OD-SAVs

We now turn to examine the scenario where PAVs follow the UE routing and OD-SAVs follow CN routing (termed as the joint mixed equilibrium). The CN routing minimizes the total travel time of all OD-SAVs that are managed by the same operator, which follows the mixed traffic equilibrium in the literature (Harker, 1988; Yang et al., 2007). We firstly formulate the joint mixed equilibrium, and then discuss the equilibrium properties and solution approach.

3.2.1. Joint mixed equilibrium formulation

The joint mixed equilibrium differs from the joint user equilibrium in the sense that OD-SAVs will follow CN routing (different OD-SAV routing model). The feasible set Φ is still defined by constraints in Eqs. (7)-(9). Moreover, PAV elastic demand equilibrium in Eq. (10), OD-SAV elastic demand equilibrium in Eq. (11), PAV parking choice equilibrium in Eq. (12), route choice equilibrium for PAV in Eq. (13) still hold. Different from UE routing based on Eq. (13), for OD-SAVs, we now have the following route choice formulation.

(OD-SAV route choice equilibrium) Given the OD-SAV flow y_{rs}, the route choice problem of OD-SAVs is to solve the following problem:

$$\underset{\boldsymbol{x}^b}{Min} \sum_{e \in E} t_e \left(x_e^a + x_e^b \right) x_e^b, \tag{19}$$

where the PAV flow in the network x_e^a is taken as given. As discussed in Yang et al. (2007), the equivalent VI formulation of the optimization problem in Eq. (19) can be expressed as:

$$\sum_{e \in E} \left[t_e \left(x_e^* \right) + x_e^{b,*} t_e' \left(x_e^* \right) \right] \left(x_e^b - x_e^{b,*} \right) \geq 0. \tag{20}$$

Combining the conditions in Eq. (10), Eq. (11), Eq. (12), Eq. (13) and Eq. (20), we have the joint mixed equilibrium, subject to the constraints of Φ that are defined in Eqs. (7)-(9).

3.2.2. VI formulation of the joint mixed equilibrium

Similarly, we can develop the VI formulation for the joint mixed equilibrium with respect to PAV demand $\boldsymbol{q^a} = \{q_{rs}^a\}$, OD-SAV demand $\boldsymbol{q^b} = \left\{q_{rs}^b\right\}$, PAV parking choice $\boldsymbol{q_p} = \left\{q_{rs,p}^a\right\}$, link flow pattern $\boldsymbol{x^a} = \{x_e^a\}$ and $\boldsymbol{x^b} = \left\{x_e^b\right\}$ as below (Kinderlehrer & Stampacchia, 2000).

Proposition 3.7. *The PAV demand, OD-SAV demand, PAV parking choice, and link flow pattern* $(\boldsymbol{q^{a,*}}, \boldsymbol{q^{b,*}}, \boldsymbol{q_p^*}, \boldsymbol{x^{a,*}}, \boldsymbol{x^{b,*}})$ *reaches the joint mixed equilibrium defined by Eq. (10), Eq. (11), Eq. (12), Eq. (13) and Eq. (20) if and only if it solves the following VI problem:*

$$\begin{aligned} &\sum_{(r,s)\in M} \sum_{p} c_{rs,p}^{a,*} (q_{rs,p}^a - q_{rs,p}^{a,*}) - \sum_{(r,s)\in M} f_{rs}^{a,-1} \left(q_{rs}^{a,*} \right) \left(q_{rs}^a - q_{rs}^{a,*} \right) + \sum_{e \in E} t_e \left(x_e^* \right) \left(x_e^a - x_e^{a,*} \right) \\ &- \sum_{(r,s)\in M} f_{rs}^{b,-1} \left(q_{rs}^{b,*} \right) \left(q_{rs}^b - q_{rs}^{b,*} \right) + \sum_{e \in E} \left[t_e \left(x_e^* \right) + x_e^{b,*} t_a' \left(x_e^* \right) \right] \left(x_e^b - x_e^{b,*} \right) \geq 0, \end{aligned} \tag{21}$$

subject to $(\boldsymbol{q^a}, \boldsymbol{q^b}, \boldsymbol{q_p}, \boldsymbol{x^a}, \boldsymbol{x^b}) \in \Phi$.

Proof. The proof is similar to that of the joint user equilibrium in Proposition 3.1, which is omitted. □

Given the PAV demand $\boldsymbol{q^a}$ and the parking choice $\boldsymbol{q_p}$, the joint mixed equilibrium reduces to a traditional fixed demand deterministic mixed equilibrium with UE travelers and CN travelers (Harker, 1988; Yang et al., 2007). Under the assumption of convex and strictly increasing travel time function introduced in Section 2, the uniqueness of the link flow pattern of joint mixed equilibrium is not guaranteed. If we further assume that the link travel time function $t_e(x_e)$ is linearly increasing with link flow x_e, the uniqueness of PAV demand pattern $\boldsymbol{q^a}$, OD-SAV demand pattern $\boldsymbol{q^b}$, link flow pattern $(\boldsymbol{x^a}, \boldsymbol{x^b})$ and parking occupancy rate $\boldsymbol{\mu} = \left\{\mu_p\right\}$ can be proved. Note that the linearity assumption of travel time function is only used to prove Proposition 3.8. The analysis and results in other parts of the paper do not rely on this assumption.

Proposition 3.8. *At the joint mixed equilibrium, the PAV demand pattern* $\boldsymbol{q^{a,*}}$*, the OD-SAV demand pattern* $\boldsymbol{q^{b,*}}$*, the parking occupancy rate* $\boldsymbol{\mu^*} = \left\{\mu_p^*\right\}$ *at all parking locations and the link flow pattern* $\left(\boldsymbol{x^{a,*}}, \boldsymbol{x^{b,*}}\right)$ *are unique, if the link travel time function* $t_e(x_e)$ *is linear and monotonically increasing with the link flow* x_e *.*

Proof. The proof is similar to those for Propositions 3.2-3.4, which is omitted here. □

Proposition 3.7 states the equivalency between the VI formulation in Eq. (21) and the joint mixed equilibrium. Proposition 3.8 discusses the uniqueness of the PAV demand $\boldsymbol{q^{a,*}}$, OD-SAV demand $\boldsymbol{q^{b,*}}$, parking occupancy rate $\boldsymbol{\mu^*}$ and link flow patterns of OD-SAV and PAV, i.e., $\left(\boldsymbol{x^{a,*}}, \boldsymbol{x^{b,*}}\right)$ under a linear and strictly increasing link travel time function. In the numerical studies, we will further compare the joint user equilibrium and the joint mixed equilibrium.

3.2.3. Solution procedure for the joint mixed equilibrium

Algorithm 2 Solution procedure for the joint mixed equilibrium

1: Initialization

(i) Set iteration number $n = 0$, traffic flow pattern $\boldsymbol{x_{(0)}} = 0$ and initialize PAV demand pattern $\boldsymbol{q^{a}_{(0)}}$;

(ii) Calculate the travel cost of PAVs denoted by $c^{a}_{rs,p,(0)}$ according to the free flow traffic pattern $\boldsymbol{x_{(0)}} = 0$, and then derive the parking choice $\boldsymbol{q_{p,(0)}}$ (based on the PAV demand $\boldsymbol{q^{a}_{(0)}}$) according to the minimal travel and parking cost subject to parking capacity constraints.

2: Traffic assignment

(i) Set $j = 1$ and $\boldsymbol{\gamma_{(j)}} = \boldsymbol{x_{(n)}}$, calculate the parking trip integrated PAV travel demand $\boldsymbol{Q_{(n)}} = \left\{Q^{a}_{rs,(n)}\right\}$ according to Eq. (6);

(ii) Assign the PAV demand $\boldsymbol{Q_{(n)}}$ based on the minimal travel time according to the existing traffic flow $\boldsymbol{\gamma_{(j)}}$, where the PAV link pattern can be derived as $\boldsymbol{l^{a}_{(j+1)}} = \left\{l^{a}_{e,j+1}\right\}$;

(iii) Assign the OD-SAV flow $\boldsymbol{y} = \{y_{rs}\}$ by applying the all-or-nothing method on the basis of the minimal partial marginal travel time (CN routing), where the OD-SAV link flow pattern is denoted as $\boldsymbol{l^{b}_{(j+1)}} = \left\{l^{b}_{e,j+1}\right\}$. Then, the link flow can be represented as $\boldsymbol{l_{j+1}} = \boldsymbol{l^{a}_{(j+1)}} + \boldsymbol{l^{b}_{(j+1)}}$;

($iiii$) Update the traffic flow pattern denoted as $\boldsymbol{\gamma_{(j+1)}} = \frac{j}{j+1}\boldsymbol{\gamma_{(j)}} + \frac{1}{j+1}\boldsymbol{l_{(j+1)}}$;

The link flow convergence criterion is defined as follows:

$$\eta_{m,x} = \frac{\sqrt{\sum\limits_{e\in E}\left(\gamma_{e,(j+1)} - \gamma_{e,(j)}\right)^{2}}}{\sum\limits_{e\in E}\gamma_{e,(j)}}. \tag{22}$$

Let ϵ_x represent a sufficiently small threshold value. If $\eta_{m,x} \leq \epsilon_x$, the link flow pattern converges, then we set $\boldsymbol{x_{(n+1)}} = \boldsymbol{\gamma_{(j)}}$ and go to Step 3, otherwise set $j = j + 1$ and go to Step 2(ii).

3: Updating the parking choice and PAV travel cost

(i) Update the travel cost of PAVs $c^{a}_{rs,p,(n+1)}$ according to the traffic flow pattern $\boldsymbol{x_{(n+1)}}$, then calculate the PAV demand $\boldsymbol{k^{a}_{(n+1)}} = \left\{f^{a}_{rs}\left(c^{a}_{rs,(n+1)}\right)\right\}$ based on the minimal route cost $c^{a}_{rs,(n+1)} = min\left\{c^{a}_{rs,p,(n+1)}\right\}$;

(ii) Calculate the parking choice $\boldsymbol{m_{p,(n+1)}}$ by assigning the PAV demand $\boldsymbol{k^{a}_{(n+1)}}$ to the parking location using all-or-nothing method based on the minimal travel cost $c^{a}_{rs,(n+1)}$;

(iii) Update the PAV demand and parking choice by using the method of successive average (MSA): $\boldsymbol{q^{a}_{(n+1)}} = \frac{n}{n+1}\boldsymbol{q^{a}_{(n)}} + \frac{1}{n+1}\boldsymbol{k^{a}_{(n+1)}}$, $\boldsymbol{q_{p,(n+1)}} = \frac{n}{n+1}\boldsymbol{q_{p,(n)}} + \frac{1}{n+1}\boldsymbol{m_{p,(n+1)}}$.

4: Convergence criterion

The total relative gap on each vector for iteration n is calculated as follows:

$$\eta_{m,p} = \frac{\sqrt{\sum\limits_{(r,s)\in M}\left(q^{a}_{rs,(n+1)} - q^{a}_{rs,(n)}\right)^{2}}}{\sum\limits_{(r,s)\in M} q^{a}_{rs,(n)}} + \frac{\sqrt{\sum\limits_{(r,s)\in M}\sum\limits_{p}\left(q^{a}_{rs,p,(n+1)} - q^{a}_{rs,p,(n)}\right)^{2}}}{\sum\limits_{(r,s)\in M}\sum\limits_{p} q^{a}_{rs,p,(n)}}. \tag{23}$$

If $\eta_{m,p} \leq \epsilon_p$, where ϵ_p represents a sufficiently small constant, the algorithm terminates and we can calculate the OD-SAV demand $\boldsymbol{q^{b}} = \left\{q^{b}_{rs}\right\}$ based on the link flow pattern, otherwise $n = n + 1$ and then go to Step 2.

As discussed earlier, the joint mixed equilibrium differs from the joint user equilibrium in terms of the OD-SAV routing principle, where OD-SAVs seek the route with minimal partial marginal travel time that corresponds to the partial marginal link travel time $t_e(x_e) + x^{b}_{e}t'_{e}(x_e)$ given in Eq. (20). The remainder of the joint mixed equilibrium is similar to that of the joint user equilibrium. Therefore, the solution procedure for the joint mixed equilibrium is very similar to that for the joint user equilibrium, except that now the OD-SAV traffic assignment is based on the partially marginal social travel time using $t_e(x_e) + x^{b}_{e}t'_{e}(x_e)$ as the link travel time function to determine the shortest path, rather than using $t_e(x_e)$ in the UE (Harker, 1988; Van Vuren et al., 1990; Yang et al., 2007). The solution procedure to solve the mixed equilibrium is presented in Algorithm 2. Note that in Step 1(*ii*) and Step 3(*ii*) of Algorithm 2, the parking flow assignment subject to parking capacity constraints is the same as that in Algorithm 1, i.e., solving the linear programming model in Eqs. (17)-(18).

4. Upper-level problem: OD-SAV ride service fare and frequency

In this section, we analyze the OD-SAV operator's pricing and OD-SAV flow (service frequency) for profit-maximization and social welfare-maximization, respectively, which is subject to the joint user equilibrium or the joint mixed equilibrium. For each OD pair, the operator determines the trip fare F_{rs} and OD-SAV flow y_{rs}, where the latter term represents the service intensity per unit time, i.e., the service frequency. The OD-SAV flow includes the vehicle repositioning trips by considering the flow conservation conditions. The more specific operational level decisions such as the scheduling, parking, and charging of individual vehicles are not considered. It is assumed that the fleet size and parking availability of OD-SAVs are sufficient to support the operations of the OD-SAV service.

4.1. Profit-maximization

We consider that the OD-SAV operator controls OD-SAVs serving all the OD pairs and aims to maximize its profit when choosing the trip fare F_{rs} and the OD-SAV flow y_{rs} for each OD pair (r, s). The OD-SAV operator's problem is as follows:

$$\underset{\boldsymbol{F},\boldsymbol{y}\geq\boldsymbol{0}}{Max}\quad \pi = \sum_{(r',s')\in M} F_{r's'}q^b_{r's'} - \psi\sum_{e\in E} x^b_e t_e\left(x_e\right) - \zeta\sum_{(r',s')\in M} y_{r's'}, \tag{24a}$$

$$\text{subject to:}\quad \sum_{\{j:(i,j)\in M\}} y_{ij} - \sum_{\{j:(j,i)\in M\}} y_{ji} = 0, \forall i\in R\cup S, \tag{24b}$$

where the OD-SAV demand (OD specific) $\left\{q^b_{rs}\right\}$ and link flow $\{x_e\}$ are governed by either the joint user equilibrium in Section 3.1 or the joint mixed equilibrium in Section 3.2. In Eq. (24a), π is the OD-SAV operator's profit; and on the right-hand side, the first term $\sum_{(r',s')\in M} F_{r's'}q^b_{r's'}$ is the total fare collected from OD-SAV travelers; the second term $\psi\sum_{e\in E} x^b_e t_e\left(x_e\right)$ is the total operation cost associated with the OD-SAVs and ψ is the operation cost per unit travel time for each OD-SAV; the third term $\zeta\sum_{(r',s')\in M} y_{r's'}$ is the total ownership cost for OD-SAV flows. The constraints in Eq. (24b) govern the OD-SAV flow conservation at each origin or destination node $i\in R\cup S$, where $\{j:(i,j)\in M\}$ represents all the destination nodes of the OD pairs in the OD set M, where the corresponding origin is node i. Through Eq. (24b), the OD-SAV inflow and outflow should be balanced at each origin/destination node, where the repositioning trips (with small number of passengers or empty trips) are included.

Based on Eq. (24). we can write down the corresponding Lagrangian function as follows:

$$L_\pi\left(\boldsymbol{F},\boldsymbol{y},\boldsymbol{\kappa}\right) = \pi + \sum_{i\in R\cup S}\kappa_i\left(\sum_{\{j:(i,j)\in M\}} y_{ij} - \sum_{\{j:(j,i)\in M\}} y_{ji}\right), \tag{25}$$

where $\boldsymbol{\kappa} = \{\kappa_i, i\in R\cup S\}$ is the Lagrangian multiplier associated with the constraint in Eq. (24b). Moreover, as mentioned in the above, OD-SAV demand (OD specific) $\left\{q^b_{rs}\right\}$ and link flow $\{x_e\}$ are governed by either the joint user equilibrium or the joint mixed equilibrium (i.e., they vary with $\boldsymbol{F}$ and $\boldsymbol{y}$).

To allow analytical derivations in order to generate some further understanding, we assume that the equilibrium solution is (at least locally) differentiable with respect to the operation strategies. Based on Eq. (25), the first-order optimality conditions (FOCs) for interior solutions can be derived as follows:

$$\frac{\partial L_\pi}{\partial F_{rs}} = q^b_{rs} + \sum_{(r',s')\in M}\left(F_{r's'}\frac{\partial q^b_{r's'}}{\partial F_{rs}}\right) - \psi\sum_{e\in E}\left(t_e\left(x_e\right) + x^b_e t'_e\left(x_e\right)\right)\frac{\partial x^b_e}{\partial F_{rs}} - \psi\sum_{e\in E} x^b_e t'_e\left(x_e\right)\frac{\partial x^a_e}{\partial F_{rs}} = 0, \tag{26a}$$

$$\frac{\partial L_\pi}{\partial y_{rs}} = \sum_{(r',s')\in M} F_{r's'}\frac{\partial q^b_{r's'}}{\partial y_{rs}} - \psi\sum_{e\in E}\left(t_e\left(x_e\right) + x^b_e t'_e\left(x_e\right)\right)\frac{\partial x^b_e}{\partial y_{rs}} - \psi\sum_{e\in E} x^b_e t'_e\left(x_e\right)\frac{\partial x^a_e}{\partial y_{rs}} - \zeta + \kappa_r - \kappa_s = 0, \tag{26b}$$

$$\frac{\partial L_\pi}{\partial \kappa_i} = \sum_{\{j:(i,j)\in M\}} y_{ij} - \sum_{\{j:(j,i)\in M\}} y_{ji} = 0. \tag{26c}$$

On the RHS of Eq. (26a), the marginal change in total fare given a marginal increase in F_{rs} is $q_{rs}^{b}+\sum_{(r',s')\in M}\left(F_{r's'}\frac{\partial q_{r's'}^{b}}{\partial F_{r's'}}\right)$. The third term $\psi\sum_{e\in E}\left(t_e\left(x_e\right)+x_e^{b}t_e'\left(x_e\right)\right)\frac{\partial x_e^{b}}{\partial F_{rs}}$ is the marginal operation cost due to the marginal OD-SAV flow change. The fourth term $\psi\sum_{e\in E}x_e^{b}t_e'\left(x_e\right)\frac{\partial x_e^{a}}{\partial F_{rs}}$ is the marginal operation cost due to the marginal PAV flow change. Eq. (26a) says that when there is a marginal change in trip fare, the marginal change in total fare should offset the summation of marginal changes in operation cost.

In Eq. (26b), the marginal change in total fare given a marginal increase in y_{rs} is $\sum_{(r',s')\in M}F_{r's'}\frac{\partial q_{r's'}^{b}}{\partial y_{r's'}}$; the marginal operation cost induced by a marginal OD-SAV flow change is $\psi\sum_{e\in E}\left(t_e\left(x_e\right)+x_e^{b}t_e'\left(x_e\right)\right)\frac{\partial x_e^{b}}{\partial F_{rs}}$; the marginal operation cost induced by a marginal PAV flow change is $\psi\sum_{e\in E}x_e^{b}t_e'\left(x_e\right)\frac{\partial x_e^{a}}{\partial F_{rs}}$; the marginal OD-SAV flow ownership cost is ζ; and κ_r is the effect of a marginal increase of OD-SAV outflow at node r (due to a marginal change in y_{rs}), and κ_s is the effect of a marginal increase of OD-SAV inflow at node s (due to a marginal change in y_{rs}). Eq. (26b) states that the marginal change in total fare should offset the summation of marginal changes in operation cost, marginal flow ownership cost and the effect of marginal changes in OD-SAV outflow/inflow when there is a marginal change in OD-SAV flow.

Eq. (26c) is the OD-SAV flow conservation condition for each node $i\in R\cup S$.

4.2. Social welfare-maximization

We now further discuss the problem of a OD-SAV operator that maximizes social welfare when choosing trip fare and OD-SAV flow (OD-specific). The social welfare-maximization problem (SW is the social welfare) can be expressed as follows:

$$\underset{\boldsymbol{F},\boldsymbol{y}\geq\boldsymbol{0}}{Max}\;SW=\sum_{(r',s')\in M}\left(\int_0^{q_{r's'}^{a}}f_{r's'}^{a,-1}(z)dz+\int_0^{q_{r's'}^{b}}f_{r's'}^{b,-1}(z)dz\right)-\sum_{(r',s')\in M}q_{r's'}^{a}c_{r's'}^{a}-\sum_{(r',s')\in M}q_{r's'}^{b}c_{r's'}^{b}$$
$$+\sum_{(r',s')\in M}q_{r's'}^{b}F_{r's'}-\sum_{(r',s')\in M}\zeta y_{r's'}-\psi\sum_{e\in E}x_e^{b}t_e\left(x_e\right),\tag{27a}$$
$$\text{subject to:}\quad\sum_{\{j:(i,j)\in M\}}y_{ij}-\sum_{\{j:(j,i)\in M\}}y_{ji}=0,\forall i\in R\cup S.\tag{27b}$$

In the social welfare formulation, the first term $\sum_{(r',s')\in M}\left(\int_0^{q_{r's'}^{a}}f_{r's'}^{a,-1}(z)dz+\int_0^{q_{r's'}^{b}}f_{r's'}^{b,-1}(z)dz\right)$ measures the total willingness to pay (benefit) for PAV and OD-SAV travelers; the second and third terms are the total travel cost respect to PAV and OD-SAV travelers, i.e., $\sum_{(r',s')\in M}q_{r's'}^{a}c_{r's'}^{a}$ and $\sum_{(r',s')\in M}q_{r's'}^{b}c_{r's'}^{b}$; the term $\sum_{(r',s')\in M}q_{r's'}^{b}F_{r's'}-\sum_{(r',s')\in M}\zeta y_{r's'}-\psi\sum_{e\in E}x_e^{b}t_e\left(x_e\right)$ denotes OD-SAV ride service operator's profit, where $\sum_{(r',s')\in M}q_{r's'}^{b}F_{r's'}$ is the total fare, $\sum_{(r',s')\in M}\zeta y_{r's'}$ is the OD-SAV flow ownership cost, and $\psi\sum_{e\in E}x_e^{b}t_e\left(x_e\right)$ is the OD-SAV operation cost.

Similar to profit-maximization problem, the demand (OD-SAV and PAV), parking choice and link flow pattern are governed by either the joint user equilibrium in Section 3.1 or joint mixed equilibrium in Section 3.2. Similarly, the Lagrangian function in relation to Eq. (27) can be written as follows:

$$L_{SW}\left(\boldsymbol{F},\boldsymbol{y},\boldsymbol{\kappa}\right)=SW+\sum_{i\in R\cup S}\kappa_i\left(\sum_{\{j:(i,j)\in M\}}y_{ij}-\sum_{\{j:(j,i)\in M\}}y_{ji}\right),\tag{28}$$

where $\boldsymbol{\kappa} = \{\kappa_i, i \in R \cup S\}$ is the Lagrangian multiplier. We then can derive the FOCs:

$$\frac{\partial L_{SW}}{\partial F_{rs}} = \left[\sum_{(r',s')\in M} F_{r's'} \frac{\partial q^b_{r's'}}{\partial F_{rs}} + q^b_{rs} - \psi \sum_{e\in E} \left(t_e(x_e) + x^b_e t'_e(x_e)\right) \frac{\partial x^b_e}{\partial F_{rs}} - \psi \sum_{e\in E} x^b_e t'_e(x_e) \frac{\partial x^a_e}{\partial F_{rs}}\right] - \sum_{(r',s')\in M} q^a_{r's'} \frac{\partial c^a_{r's'}}{\partial F_{rs}} - \sum_{(r',s')\in M} q^b_{r's'} \frac{\partial c^b_{r's'}}{\partial F_{rs}} = 0, \tag{29a}$$

$$\frac{\partial L_{SW}}{\partial y_{rs}} = \left[\sum_{(r',s')\in M} F_{r's'} \frac{\partial q^b_{r's'}}{\partial y_{rs}} - \psi \sum_{e\in E} \left(t_e(x_e) + x^b_e t'_e(x_e)\right) \frac{\partial x^b_e}{\partial y_{rs}} - \psi \sum_{e\in E} x^b_e t'_e(x_e) \frac{\partial x^a_e}{\partial y_{rs}} - \zeta\right] - \sum_{(r',s')\in M} q^a_{r's'} \frac{\partial c^a_{r's'}}{\partial y_{rs}} - \sum_{(r',s')\in M} q^b_{r's'} \frac{\partial c^b_{r's'}}{\partial y_{rs}} + \kappa_r - \kappa_s = 0, \tag{29b}$$

$$\frac{\partial L_{SW}}{\partial \kappa_i} = \sum_{\{j:(i,j)\in M\}} y_{ij} - \sum_{\{j:(j,i)\in M\}} y_{ji} = 0. \tag{29c}$$

In Eq. (29a), the marginal change in profit given a marginal increase in F_{rs} (the first term on the RHS of Eq. (29a)) is associated with the marginal total fare $\sum_{(r',s')\in M} F_{r's'} \frac{\partial q^b_{r's'}}{\partial F_{rs}} + q^b_{rs}$, the marginal operation cost induced by marginal OD-SAV flow change $\psi \sum_{e\in E} \left(t_e(x_e) + x^b_e t'_e(x_e)\right) \frac{\partial x^b_e}{\partial F_{rs}}$, and the marginal operation cost induced by marginal PAV flow change $\psi \sum_{e\in E} x^b_e t'_e(x_e) \frac{\partial x^a_e}{\partial F_{rs}}$. The marginal change in consumer surplus induced by a marginal change of fare F_{rs} equals the sum of marginal change in OD-SAV travelers' surplus $\sum_{(r',s')\in M} q^a_{r's'} \frac{\partial c^a_{r's'}}{\partial F_{rs}}$ and marginal change in PAV travelers' surplus $\sum_{(r',s')\in M} q^b_{r's'} \frac{\partial c^b_{r's'}}{\partial F_{rs}}$. Eq. (29a) says the marginal change in operator's profit should offset the marginal change in the consumer surplus of PAV and OD-SAV travelers.

In Eq. (29b), the marginal profit given a marginal increase in y_{rs} is associated with the marginal total fare $\sum_{(r',s')\in M} F_{r's'} \frac{\partial q^b_{r's'}}{\partial y_{r's'}}$, the marginal operation cost induced by a marginal vehicle flow change $\psi \sum_{e\in E} \left(t_e(x_e) + x^b_e t'_e(x_e)\right) \frac{\partial x^b_e}{\partial y_{rs}}$, the marginal operation cost induced by a marginal PAV flow change $\psi \sum_{e\in E} x^b_e t'_e(x_e) \frac{\partial x^a_e}{\partial y_{rs}}$, and the marginal OD-SAV flow ownership cost ζ. The term $\sum_{(r',s')\in M} q^a_{r's'} \frac{\partial c^a_{r's'}}{\partial y_{rs}}$ and $\sum_{(r',s')\in M} q^b_{r's'} \frac{\partial c^b_{r's'}}{\partial y_{rs}}$ denote the marginal change in consumers' surplus with respect to PAV and OD-SAV travelers respectively. Similarly, $\kappa_r - \kappa_s$ represents the marginal increase of OD-SAV outflow and inflow for the node r and node s due to a marginal change in y_{rs}. Eq. (29b) says that when there is a marginal change in OD-SAV flow, the marginal change in total profit should offset the summation of marginal changes in consumer surplus with respect to OD-SAV and PAV travelers and the marginal change of inflow and outflow for the OD pair.

Eq. (29c) is the OD-SAV flow conservation condition for each node $i \in R \cup S$.

By comparing the FOCs for profit-maximization and social welfare-maximization, we can see that the social welfare maximizing operator concerns the profit of the OD-SAV ride service operator and the consumer surplus of both PAV and OD-SAV travelers, while a profit maximizing operator concerns only the total fare and operation cost.

4.2.1. Solution procedure for the bi-level problem

We now present the solution procedures to solve the OD-SAV operator's problem (service fare and OD-SAV flow) under profit-maximization and social welfare-maximization subject to the joint user equilibrium or the joint mixed equilibrium defined in Section 3.1 and Section 3.2, respectively. Note that the optimal service fare and OD-SAV flow may not be unique. The general idea to solve the above problem is as follows. First, we choose the OD-SAV service fare and OD-SAV flow, and then calculate the joint user equilibrium or the joint mixed equilibrium by the solution procedures in Algorithm 1 or 2 (described in Step 1&2 in Algorithm 3). Second, we update the OD-SAV service fare and OD-SAV flow according to the information of the derivatives with respect to fare and OD-SAV flow, respectively, while taking the joint network equilibrium solution as given (described in Step 3&4 in Algorithm 3). Note that for each iteration of Algorithm 3, the lower-level convergence criterion should be satisfied. This method is similar to the gradient descent method in the literature and the solution might converge to a local optimum. If the convergence criterion is not met, we repeat the above whole procedure to update the equilibrium solution and the OD-SAV service fare and OD-SAV flow. The detailed solution procedure for the bi-level problem is as follows.

Algorithm 3 Solution procedure for the bi-level problem

1: Initialization: set the iteration number $n = 0$ and then set initial feasible trip fares $\boldsymbol{F_{(0)}} = \{F_{rs,(0)}\}$ and OD-SAV flows $\boldsymbol{y_{(0)}} = \{y_{rs,(0)}\}$ for all OD pairs;

2: Given the trip fare $\boldsymbol{F_{(n)}}$ and OD-SAV flow $\boldsymbol{y_{(n)}}$, implement Algorithm 1 (or Algorithm 2) to solve the lower-level joint user equilibrium (or joint mixed equilibrium) and derive the PAV demand $\boldsymbol{q^{a,*}_{(n)}}$, PAV parking choice $\boldsymbol{q^{*}_{p,(n)}}$ and link flows $\boldsymbol{x^{*}_{(n)}}$, where OD-SAV and PAV link flows are denoted by $\boldsymbol{x^{a,*}_{(n)}}$ and $\boldsymbol{x^{b,*}_{(n)}}$, respectively;

3: Given the PAV demand $\boldsymbol{q^{a,*}_{(n)}}$, PAV parking choice $\boldsymbol{q^{*}_{p,(n)}}$ and link flow denoted by $\boldsymbol{x^{*}_{(n)}}$, we solve the operator's optimization problem, i.e., profit-maximization in Eq. (24) and social welfare-maximization in Eq. (27). The solution with respect to trip fare $\boldsymbol{g_{(n+1)}} = \{g_{rs,(n+1)}\}$ and OD-SAV flow $\boldsymbol{z_{(n+1)}} = \{z_{rs,(n+1)}\}$ can be obtained.

4: Update the operator's optimal solutions denoted by $F_{rs,(n+1)} = \frac{n}{n+1}F_{rs,(n)} + \frac{1}{n+1}g_{rs,(n+1)}, \forall (r,s) \in M$ and $y_{rs,(n+1)} = \frac{n}{n+1}y_{rs,(n)} + \frac{1}{n+1}z_{rs,(n+1)}, \forall (r,s) \in M$.

5: Convergence criterion:

$$\eta_s = \frac{\sqrt{\sum\limits_{(r,s)\in M}\left(F_{rs,(n+1)} - F_{rs,(n)}\right)^2}}{\sum\limits_{(r,s)\in M} F_{rs,(n)}} + \frac{\sqrt{\sum\limits_{(r,s)\in M}\left(y_{rs,(n+1)} - y_{rs,(n)}\right)^2}}{\sum\limits_{(r,s)\in M} y_{rs,(n)}}. \tag{30}$$

Let ϵ_s represent a sufficiently small threshold value. If $\eta_s \leq \epsilon_s$, the solution procedure converges and terminates, otherwise set $n = n + 1$, and then go to Step 2.

5. Numerical studies

This section presents numerical studies to further illustrate the proposed model in the Hong Kong context. In the following analysis, we will examine and compare four scenarios: (i) profit-maximization under the joint user equilibrium (P-JUE); (ii) social welfare-maximization under the joint user equilibrium (SW-JUE); (iii) profit-maximization under the joint mixed equilibrium (P-JME); (iv) social welfare-maximization under the joint mixed equilibrium (SW-JME). Furthermore, we examine the effects of different parking supplies (i.e., parking fee and parking capacity) on the network performance. The numerical experiments in this paper are designed and conducted using MATLAB R2021b on an Intel (R) core (TM)-I7(Dell) CPU 3.2 GHZ with 4 GB RAM and 500 GB hard disk. The analysis period of the numerical experiment is one hour.

5.1. The Hong Kong network and numerical setting

The numerical study is based on an aggregate network representation of Hong Kong. Eighteen administrative regions in Hong Kong are considered, which are numbered as follows: (1) Islands District, (2) Kwai Tsing District, (3) North District, (4) Sai Kung District, (5) Sha Tin District, (6) Tai Po District, (7) Tsuen Wan District, (8) Tuen Mun District, (9) Yuen Long District, (10) Kowloon City District, (11) Kwun Tong District, (12) Sham Shui Po District, (13) Wong Tai Sin District, (14) Yau Tsim Mong District, (15) Central & Western District, (16) Eastern District, (17) Southern District, and (18) Wan Chai District. Each administrative region shown in Fig. 2a is taken as one node as presented in Fig. 2b. The links are derived by combining the arterial roads and expressways of the existing road network in Hong Kong between the administrative regions. The aggregate network in Fig. 2b consists of 18 nodes and 24 bi-directional links, where we set seven major parking locations, i.e., node 3, 4, 7, 8, 14, 16, 17.[3] The detailed link information (link length and link travel time) is presented in Table E.6 of Appendix E. The parking supply related parameters and OD pair information are shown in Table 1.

[3]The detailed road network information is obtained through the website DATA.GOV.HK (`https://data.gov.hk/`).

The link travel time function is set as $t_e = t_{e,0} + \xi_e x_e$, where $t_{e,0}$ is the free flow travel time and ξ_e is a positive coefficient. The demand function with respect to OD-SAV or PAV mode is set as follows: $q_{rs}^m = f_{rs}^m(c) = D_m \exp\{-\upsilon_m \cdot c\}, \forall m \in \{a, b\}$, where c is the travel cost, D_m is the potential demand for mode m and υ_m ($\upsilon_m > 0$) is the demand sensitivity parameter. With a marginal increase in travel cost, a larger value of demand sensitivity parameter υ_m implies a larger reduction in travel demand. The waiting time function of OD-SAV ride service is assumed as $w^c = \frac{\rho \cdot q_{rs}^b}{\sqrt{y_{rs}}}$, where w^c is the average waiting time for the OD-SAV ride service, and ρ is a positive coefficient. Note that the function forms and parameter values should be rigorously calibrated using real-world data, e.g., the economic, demographic and travel behavior characteristics and network topology, when the model is applied to a specific urban area. In this paper, the parameters are assumed as follows: $D_a = 8 \times 10^4$(trips/h), $D_b = 7 \times 10^4$(trips/h), $\upsilon_a = 0.12$, $\upsilon_b = 0.08$, $\rho = 0.1$, $\beta = 50$(HKD/h), $\alpha = 20$(HKD/h), the inconvenience cost of OD-SAV travel $\delta = 1.2$(HKD), PAV ownership cost $\sigma = 3.5$(HKD/trip) and OD-SAV flow ownership cost $\zeta = 5$(HKD/trip), the operation cost of each OD-SAV $\psi = 36$(HKD/h). In the convergence criterion of solution procedures, we set $\epsilon_p = \epsilon_x = 1 \times 10^{-4}$ and $\epsilon_s = 1 \times 10^{-3}$.

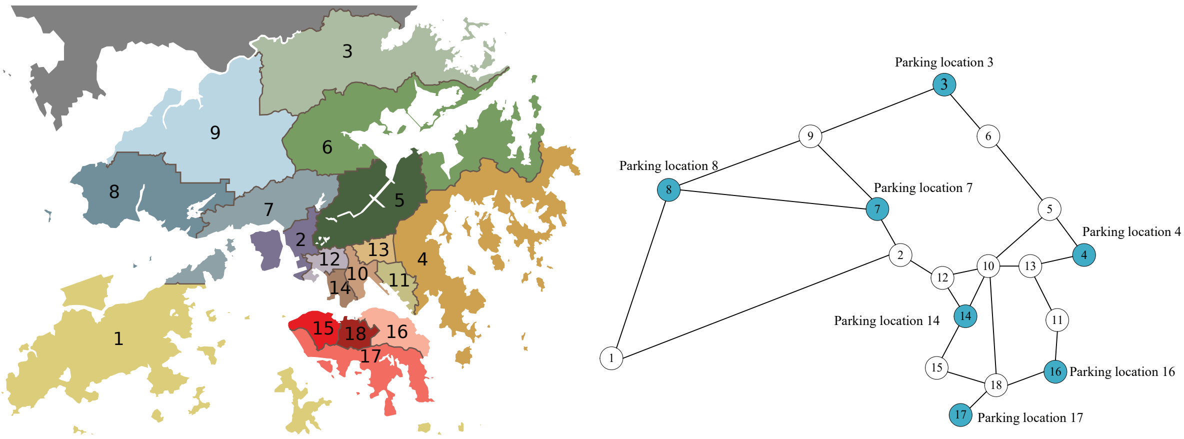

(a) Administrative regions in Hong Kong **(b)** Aggregate network presentation based on administrative regions

Fig. 2. Study area with 18 administrative regions (network nodes) in Hong Kong

Table 1 The OD and parking location information

Parking location	Node 3		Node 4		Node 7		Node 8		Node 14		Node 16		Node 17	
Parking fee (HKD)	10		12		15		10		17		17		13	
Capacity (vehicles)	14000		9000		11000		22000		8000		8500		10000	
OD pair (r, s)	1-12	1-17	2-13	3-8	3-15	4-3	5-11	5-12	6-7	7-8	8-1	8-9	8-16	9-3
	9-5	10-1	10-2	10-5	11-18	12-9	12-17	13-17	15-10	16-6	17-3	17-4	17-10	18-10

5.2. Scenario comparison

We now compare the four scenarios mentioned before (i.e., P-JUE, SW-JUE, P-JME, and SW-JME) given the numerical setting in Section 5.1. In Table 2, we present several system efficiency metrics for the four scenarios, respectively, aiming to evaluate and compare the overall network performance. The total OD-SAV flow and total PAV/OD-SAV demand are the summations of the OD-SAV flows and demands for all OD pairs in the network, respectively. The trip fares across all the OD paris are presented in Appendix E. In particular, we examine the indicator 'average OD-SAV demand-flow ratio' that equals the served OD-SAV demand divided by the OD-SAV flow for each OD pair. This indicator reflects the average utilization rate of the deployed SAVs for each OD pair, which implicitly indicates the proportion of repositioning trips or empty trips. The smaller the ratio, the less utilized the vehicles are and the more empty trips there are. The convergence of the proposed solution procedures for the upper-level problem and lower-level network equilibrium are illustrated in Fig. 3 and Fig. 4, respectively, where the gap values all approach zero over iterations. For each iteration of upper-level solution, the lower-level convergence criterion is satisfied. To save space, we do not show the lower-level convergence processes for all iterations. As an example, Fig. 4 presents the lower-level problem convergence of the last iteration of solving the upper-level problem, which corresponds to the last iteration in Fig. 3. Moreover, the lower-level solution variation with respect to the upper-level solutions in different iterations are further presented in Appendix F, where the convergence and solution variation of lower-level problem are examined. With the mentioned computation environment in Section 5, it approximately takes 14h to obtain the converged results for a single execution.

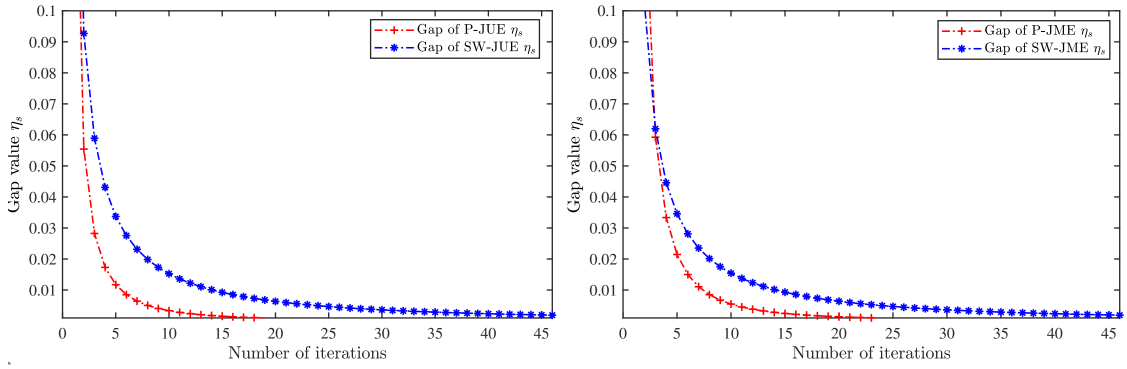

(a) Upper-level convergence under joint user equilibrium **(b)** Upper-level convergence under joint mixed equilibrium

Fig. 3. Convergence of the upper-level problem subject to lower-level equilibrium

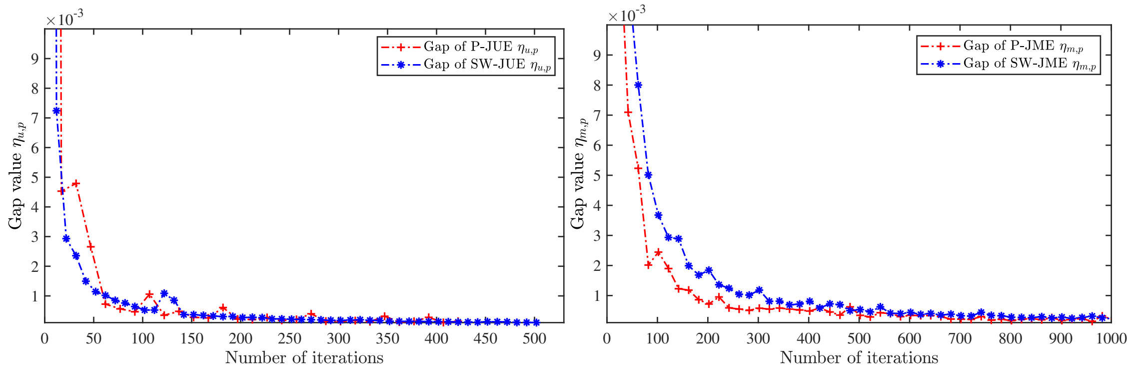

(a) Convergence of the joint user equilibrium **(b)** Convergence of the joint mixed equilibrium

Fig. 4. Convergence of the lower-level equilibrium at the last iteration of upper-level solution

As shown in Table 2, the OD-SAV ride service operator's profit is significantly lower (e..g, $-73.78 < 2.71$, $-36.47 < 119.08$), and the social welfare is larger (e.g., $5.58 > 3.51$, $7.14 > 4.68$) in SW-JUE and SW-JME when compared with P-JUE and P-JME. Also, the social welfare maximizing operator tends to reduce the trip fare and increases the OD-SAV flow (i.e., $0.15 < 8.42$, $0.15 < 8.45$ and $17469 > 4532$, $29374 > 8067$) when compared to the profit maximizing operator. In addition, the demand for PAVs is less (i.e., $59328 < 62775$, $3719 < 17333$) but can achieve a larger social welfare, indicating that less PAV trips (reduced vehicle traffic) will benefit the system. The 'average OD-SAV demand-flow ratio' reflects the average vehicle utilization of OD-SAVs, where the OD-SAV service is operated with less average OD-SAV flow but a larger vehicle utilization rate under profit-maximization with UE routing (i.e., $18.98 > 12.95$ and $162 < 624$). The parking occupancy rates at all parking locations are lower given less PAV demand. Moreover, an operator who aims to maximize the social welfare under the joint user equilibrium or joint mixed equilibrium should be subsidized to maintain break-even.

We now discuss the effect of OD-SAV routing on system efficiency metrics by comparing P-JUE and SW-JUE with P-JME and SW-JME, respectively. Table 2 shows that the profit, as well as social welfare in the joint mixed equilibrium, will be greater than that in the joint user equilibrium (e.g., 119.08 > 2.71 and 4.68 > 3.51 in P-JME and P-JUE and −36.41 > −73.78 and 7.14 > 5.58 in SW-JME and SW-JUE). Moreover, under the joint mixed equilibrium, the OD-SAV demand is larger while the PAV travel demand and the parking demand are less than those in the joint user equilibrium.

Table 2 System efficiency metrics under the four scenarios (P-JUE, SW-JUE, P-JME, and SW-JME)

Scenarios	Profit(10^4)	SW(10^6)	Total OD-SAV flow	Average trip fare (HKD)	Total OD-SAV demand	Total PAV demand	Average OD-SAV demand-flow ratio	Average OD-SAV flow
P-JUE	2.71	3.51	4532	8.42	202257	62775	18.98	162
SW-JUE	-73.78	5.58	17469	0.15	382449	59328	12.95	624
P-JME	119.08	4.68	8067	8.45	302266	17333	5.83	288
SW-JME	-36.41	7.14	29374	0.15	571915	3719	7.02	1049
Parking occupancy rate	Node 3	Node 4	Node 7	Node 8	Node 14	Node 16	Node 17	
P-JUE	0.82	1.00	0.31	0.57	1.00	1.00	1.00	
SW-JUE	0.71	1.00	0.22	0.53	1.00	1.00	1.00	
P-JME	0.13	0.38	0.09	0.18	0.43	0.22	0.19	
SW-JME	0.01	0.09	0.00	0.03	0.10	0.09	0.05	

5.3. Impact of parking supply

In this section, we numerically examine how varying the parking supply may affect the network performance, i.e., the lower-level network equilibrium and the OD-SAV ride operator's optimal operation strategy and profit, and social welfare. Specifically, we vary the parking fee and parking capacity of node 14, where node 14 is the most utilized parking node in the benchmark case presented in Table 2.

We firstly vary the parking fee of parking node 14, and Fig. 5 shows how the equilibrium parking occupancy rates at different parking locations change with the parking fee. Table 3 summarizes several system efficiency metrics under a parking fee of 22 HKD for node 14 (the benchmark case in Table 2 has a parking fee of 17 HKD for node 14). Fig. 5a shows that with the increment of node 14's parking fee, other parking nodes with a relatively high occupancy rate (e.g., node 4, 16 & 17) will only be slightly affected as the these parking nodes are almost fully utilized already. Given the increment of parking fee of node 14, the parking demand at a parking node with a relatively low occupancy rate (e.g., parking node 3, 7 & 8) tends to increase, which is partially due to the redistribution of parking demand given the more costly parking at node 14.

We now further compare different system efficiency metrics under two different parking fees (22 and 17) for node 14. By comparing that in Table 3 with the results in the benchmark case in Table 2, one can see that the social welfare decrease in all scenarios (P-JUE, SW-JUE, P-JME and SW-JME), while only the profit in P-JUE will be significantly reduced when the parking fee of node 14 is increased to 22 (HKD). This implies that the profit-driven operator (P-JUE) can be more sensitive to the change of parking fee of the most utilized parking node (node 14) when compared with the scenario with a public operator (SW-JUE). Most other metrics in the two tables are similar, which suggests that a local parking pricing change at node 14 does pose substantial change to aggregate system efficiency metrics (while the traffic and parking distributions have changed, as shown in Fig. 5a).

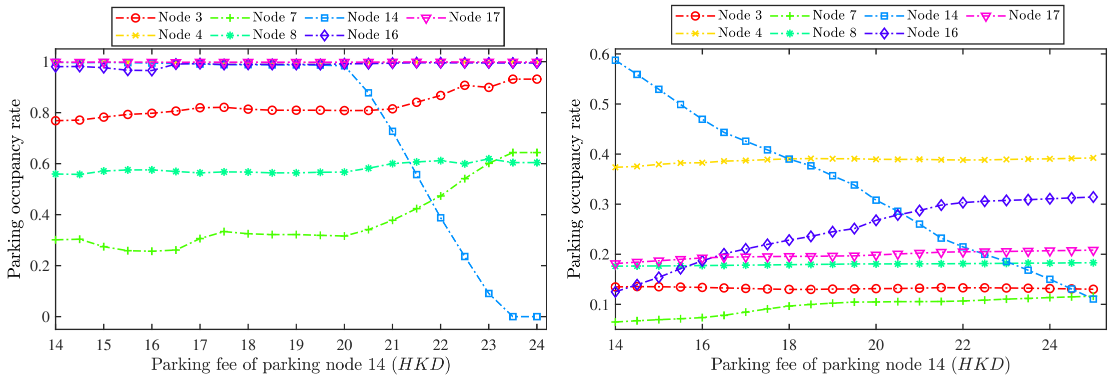

(a) Parking occupancy rate under the joint user equilibrium **(b)** Parking occupancy rate under the joint mixed equilibrium

Fig. 5. Parking occupancy rate variation with respect to parking fee of node 14

Table 3 System efficiency metrics when parking fee of node 14 is equal to 22 (HKD)

Scenarios	Profit(10^4)	SW(10^6)	Total OD-SAV flow	Average trip fare (HKD)	Total demand for OD-SAV	Total PAV demand
P-JUE	-0.23	3.21	4345	8.42	195699	61528
SW-JUE	-73.32	5.24	16745	0.15	369788	58089
P-JME	118.48	4.63	8049	8.45	301001	16881
SW-JME	-36.41	7.13	29349	0.15	571378	3640

We now vary the parking capacity of node 14. Fig. 6 shows how the parking occupancy rate varies with the variation of parking capacity of node 14 under the joint user equilibrium and the joint mixed equilibrium. Table 4 presents several system efficiency metrics when the parking capacity of node 14 is expanded to 16000 (the benchmark case in Table 2 has a parking capacity of 8000 for node 14). Fig. 6a shows that with the increment of the capacity of node 14, the parking occupancy rates at nodes 3 & 7 firstly decreases and then remains constant under the joint user equilibrium. In the benchmark case, parking at node 14 is a preferred option by many. When the capacity increases, travelers will shift to parking at node 14 (from other parking nodes, i.e., nodes 3 & 7). At the joint mixed equilibrium (Fig. 6b), since the parking occupancy rate is relatively low for all the parking nodes, increasing the capacity at node 14 does not affect parking occupancy rate at other parking locations.

We now compare the system efficiency metrics in Table 4 under a parking capacity of 16000 for node 14 with those in the benchmark case. One can see that there are observable changes under the joint user equilibrium (P-JUE and SW-JUE), while the solutions under the joint mixed equilibrium remain unchanged (consistent with observations from Fig. 6). As can be seen, the expansion of the parking capacity can benefit both the operator and the whole system in P-JUE through increasing the demand for both OD-SAV and PAV. However, a social welfare maximizing operator will require a larger subsidy (SW-JUE) in order to maintain break-even while the maximum social welfare achieved is larger.

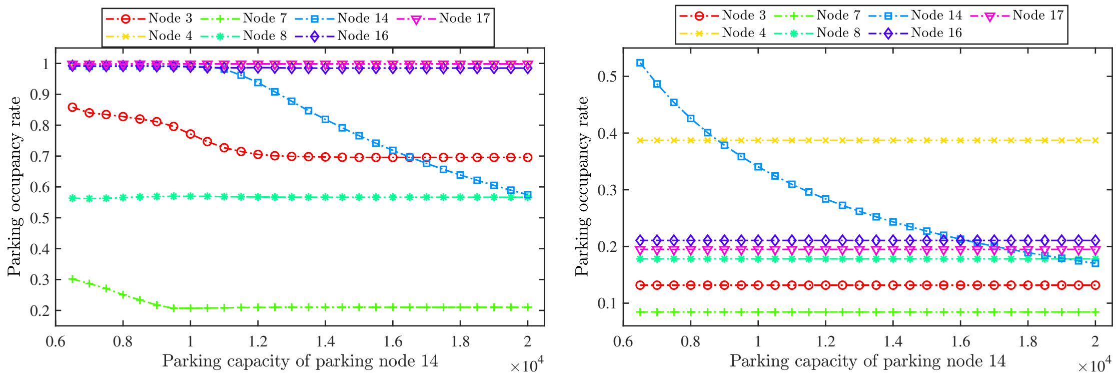

(a) Parking occupancy rate under the joint user equilibrium **(b)** Parking occupancy rate under the joint mixed equilibrium

Fig. 6. Parking occupancy rate variation with respect to parking capacity of node 14

Table 4 System efficiency metrics when capacity of node 14 is expanded to 16000

Scenarios	Profit(10^4)	SW(10^6)	Total OD-SAV flow	Average trip fare (HKD)	Total demand for OD-SAV	Total PAV demand
P-JUE	4.75	3.66	4684	8.42	206759	64098
SW-JUE	-73.90	5.69	17807	0.15	387837	60009
P-JME	119.08	4.68	8067	8.45	302266	17333
SW-JME	-36.41	7.14	29373	0.15	571897	3719

5.4. Sensitivity analysis of vehicle ownership cost

In this section, we numerically examine how the OD-SAV/PAV demand and the parking occupancy rate vary with the vehicle ownership cost σ under P-JUE and P-JME respectively.

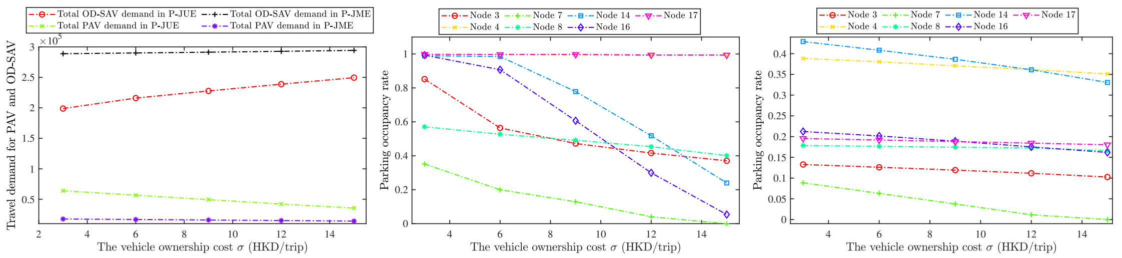

(a) OD-SAV/PAV demand with σ **(b)** Parking occupancy rate with σ in P-JUE **(c)** Parking occupancy rate with σ in P-JME

Fig. 7. Solution variation with the vehicle ownership cost σ (HKD/trip) in P-JUE or P-JME

Fig. 7 shows the variation of solutions when the vehicle ownership cost σ varies between 3 and 15 (HKD/trip). Specifically, the variations of OD-SAV/PAV demand and parking occupancy under P-JUE or P-JME are presented in Fig. 7a, Fig. 7b and Fig. 7c, respectively. The results show that with the increment of vehicle ownership cost σ, the total PAV demand will decrease and the total SAV demand will increase regardless of the route choice principles of SAVs (UE or CN). Intuitively, with more cost to acquire a vehicle, more travelers may choose the OD-SAV service instead of PAV traveling, and this will result in an increment of the OD-SAV demand. With the reduction of PAV demand due to the increasing vehicle ownership cost σ, the parking occupancy rate under P-JUE or P-JME will also decrease (as shown in Fig. 7b and Fig. 7c). However, the parking occupancy rates in P-JUE change more dramatically compared with that in P-JME. This suggests that vehicle ownership cost has less effect on the equilibrium parking occupancy rate when SAVs follow the CN routing.

6. Conclusion

In this section, we firstly summarize the main results and managerial insights of this paper through the current modeling framework and approach in Section 6.1, and then discuss the basic assumption and limitation of adopted methodology as well as the future research directions in Section 6.2.

6.1. Summary

This paper develops bi-level network equilibrium models to investigate the interaction between OD-SAVs and PAVs and the optimization of the OD-SAV ride service. The PAV travelers will determine the parking location and corresponding route choice. The OD-SAV service provided by the operator is considered similar to the shared shuttle service which serves a specific direct OD pair, and allows multiple passengers with a common OD pair to share a vehicle. At the same time, the route of OD-SAVs can be flexibly controlled by the service operator. We consider that PAVs follow UE routing while OD-SAVs may either follow UE routing or CN routing, resulting in a joint user equilibrium or joint mixed equilibrium. The uniqueness/non-uniqueness properties of the PAV/OD-SAV demand, link flow pattern, and parking occupancy rates are discussed by utilizing the proposed VI formulations for the joint user equilibrium and joint mixed equilibrium. We also examine the OD-SAV ride service operator's optimal pricing and fleet flow deployment under either profit-maximization or social welfare-maximization subject to the lower-level network equilibrium (i.e., the upper-level problem).

The results show that the PAV/OD-SAV demand pattern, link flow pattern with two types of vehicles, and parking occupancy rate at each parking location can be uniquely determined at the joint lower-level equilibrium of parking choice and travel route choice. The numerical study indicates that, when compared to a private profit-driven operator, a public OD-SAV service operator tends to serve a larger OD-SAV demand and yields a larger social welfare. However, the operator has to be subsidized in order to maintain break-even. Also, we found that under the CN routing of OD-SAVs, there will be less PAV travel demand, and less parking demand, which yields a larger social welfare and a larger profit for OD-SAV ride service when compared with UE routing (for OD-SAVs). We also found that a profit-driven OD-SAV operator following UE routing can be more sensitive to the variation of the parking supplies when compared with other scenarios (e.g., social welfare-maximization operator following CN routing). In summary, this study enhances our understanding of (i) how OD-SAVs and PAVs will interact with each other and how the interaction will further affect the network performance; (ii) how PAVs' self-driving to parking will affect travelers' travel and parking decisions; and (iii) how OD-SAV ride service should be optimized in order to achieve different economic objectives.

6.2. Limitations and future research directions

This paper takes an aggregate and static approach to characterize travel choices and network traffic assignment in the long-term equilibrium. This approach allows for analytical tractability under which we derive the analytical properties of the built equilibrium models. We consider an OD-based shared autonomous vehicle ride service operated with autonomous vehicles, which is inspired by the public transportation service and OD-based shared shuttle service in the existing transportation system. The equilibrium traffic flow for OD-SAV reflects the average service frequency. The more specific operational level decisions of OD-SAV service operator are not considered, such as the scheduling, routing, parking, charging, and the passenger assignment for individual vehicles. The main limitations and future research directions are summarized as follows:

Static and deterministic modeling approach: This paper models the network equilibrium in a static and deterministic manner. Time-dependent travel behaviors and complex interactions associated with travelers' mode, departure time, route choices are not considered. It is of our interest to further develop a dynamical model to examine the time-dependent travel and parking choices with PAV and OD-SAV, and traffic conditions and dynamics by implementing the dynamic approach following studies of Liu & Geroliminis (2017); Zhang et al. (2018a); Chen & Levin (2019); Wei et al. (2020); Narayanan et al. (2022). In a dynamic system, current decisions and choices of travelers will impact the traffic flow and system conditions, which will in turn affect future decision-making. In particular, the OD traveling and parking trips of PAV travelers are interrelated in the time dimension, and are subject to the time-varying network traffic conditions. We may also consider optimizing the parking supply and management strategies given the parking and congestion dynamics.

Elastic demand and mode choices: This study models the PAV and OD-SAV travels and elastic demands, but does not explicitly consider individual traveler's mode choice among PAV, OD-SAV and other travel alternatives, especially when there might be complex competitive and complementary relationships among the services. Even though the elastic demand function can implicitly accommodate the mode shift behavior, it renders the estimation of the demand functions for two travel options simultaneously (Graham & Glaister, 2004; Litman, 2017). A future study may explicitly address the mode shift between private and shared autonomous vehicle travels and further incorporate the multi-modality and inter-modality in a transportation system (such as those considered in Zhu et al., 2020; Zhang & Liu, 2021). It is also of our interest to compare the difference between the implicit and explicit modeling approaches in different application scenarios (Narayanan et al., 2020; Tsouros et al., 2021; Wang & Noland, 2021).

Full autonomy environment: This paper considers a full autonomy traffic system (Zhang et al., 2019b; Wang et al., 2021; Reed et al., 2022), and aims to examine travelers' traveling and parking behaviors, and how autonomous vehicles affect urban road network performance. The co-existence of human-driven vehicles and autonomous vehicles is not considered, where the flow interactions and network traffic flow patterns will be further complicated due to the behavior characteristics of humans. On the one hand, the mixed traffic might change the road capacity and affect the choices of travelers. On the other hand, the cruising for parking traffic of human-driven vehicles will also add to road network flow interaction, and systematically affect the overall network performance. In a future study, the network traffic equilibrium with mixed autonomous and human-driven vehicles can be investigated to provide insights for the transition period (Noruzoliaee et al., 2018; Wu et al., 2020; Zhang et al., 2022). The decision-making and travel behavior of human-driven vehicle travelers and the more complex flow interactions should be incorporated (Liu et al., 2014; Liu & Geroliminis, 2016; Zhang et al., 2020).

Acknowledgement. We are very grateful to the handling editor and three anonymous referees for their constructive comments that have led to a significant improvement of the paper. The work described in this paper was partially supported by the Research Grants Council of Hong Kong (No. 27202221), the National Natural Science Foundation of China (No. 72101222), The University of Hong Kong (No. 202009185002), and The Hong Kong Polytechnic University (P0039246, P0040900).

Appendix A. List of notations

Table A.5 Notational glossary

Notation	Description	Notation	Description
	Endogenous variables		**Sets**
q^a_{rs}	PAV travel demand between OD pair (r, s)	G	Network graph
$\boldsymbol{q^a}$	Vector of PAV travel demand, $\{q^a_{rs}\}$	N	Network node set
$c^a_{rs,p}$	Travel cost from origin r to parking location p via destination s at equilibrium	E	Set of link: $\{e\}$
c^b_{rs}	Travel cost from origin r to destination s for OD-SAV ride service at equilibrium	M	The OD pair set
$\boldsymbol{q^b}$	Vector of OD-SAV ride service demand, $\left\{q^b_{rs}\right\}$	M'	The parking trip integrated OD pair set
q^b_{rs}	OD-SAV ride service demand between OD pair (r, s)	R	Set of origin node: $\{r\}$
$q^a_{rs,p}$	PAV parking demand for parking location p between OD pair (r, s)	S	Set of destination node: $\{s\}$
$\boldsymbol{q_p}$	Vector of the PAV parking demand, $\left\{q^a_{rs,p}\right\}$	P	Set of parking node: $\{p\}$
$q^a_{s,p}$ $(\overline{q}^a_{rs})$	Travel demand from destination s to parking lot p	Φ	Feasible domain
Q^a_{rs}	Total demand of PAV including OD travel and self-parking between OD pair (r, s)	W_{rs}	Set of Routes for OD pair (r, s)
x_e	Flow on link $e \in E$		**Decision variables**
$\boldsymbol{x}$	Link flow vector, $\{x_e\}$	F_{rs}	Trip fare for OD-SAV ride service between OD pair (r, s)
$\boldsymbol{x^*}$	Link flow vector at equilibrium, $\{x^*_e\}$	y_{rs}	OD-SAV flow between OD pair (r, s)
x^a_e	PAV flow on link $e \in E$		**Parameters**
$\boldsymbol{x^a}$	PAV link flow vector, $\{x^a_e\}$	Z_p	Parking fee at the parking lot p
$\boldsymbol{x^{a,*}}$	PAV link flow vector at equilibrium, $\{x^{a,*}_e\}$	β	Value of time for OD traveling
x^b_e	OD-SAV flow on link $e \in E$	α	Value of time for self-parking
$\boldsymbol{x^b}$	OD-SAV link flow vector, $\left\{x^b_e\right\}$	σ	OD-SAV ride service inconvenience cost
$\boldsymbol{x^{b,*}}$	OD-SAV link flow vector at equilibrium, $\left\{x^{b,*}_e\right\}$	ζ	Ownership cost for one OD-SAV
t_e	Travel time on link a	ψ	OD-SAV unit travel time operation cost
$t_{rs,w}$	The travel time from r to s through path w, $w \in W_{rs}$	C_p	Parking capacity at parking location $p \in P$
t_{rs}	The travel time from r to s at equilibrium		
$v_{rs,w}$	Flow on path w from origin r to destination s, $w \in W_{rs}$		
$v^a_{rs,w}$	PAV flow on route w from origin r to destination s, $w \in W_{rs}$		
$v^b_{rs,w}$	OD-SAV flow on route w from origin r to destination s, $w \in W_{rs}$		
λ_p	Advanced booking cost at parking location $p \in P$		
u_p	Total parking demand on parking lot $p \in P$		
$\boldsymbol{u}$	Vector of parking occupancy rate, $\left\{u_p\right\}$		
$\boldsymbol{d}$	Vector of total parking demand, $\left\{d_p\right\}$		
d_p	Occupancy rate at parking lot $p \in P$		

Appendix B. Proof of Proposition 3.1

This appendix provides the proof of the equivalency between the joint user equilibrium defined in Eqs. (10)-(13) and the VI formulations in Eq. (14).

Proof. **Necessity: Joint user equilibrium $\implies$ VI**

We start with the first two terms of the VI formulation in Eq. (14). Based on the PAV elastic demand equilibrium in Eq. (10), parking choice equilibrium conditions in Eq. (12), we can easily derive the following:

$$\left(c^{a,*}_{rs,p} - c^a_{rs}\right) q^{a,*}_{rs,p} = 0; \left(c^{a,*}_{rs,p} - c^a_{rs}\right) q^a_{rs,p} \geq 0, \tag{B.1a}$$

$$\left(c^a_{rs} - f^{a,-1}_{rs}\left(q^{a,*}_{rs}\right)\right) q^{a,*}_{rs} = 0; \left(c^a_{rs} - f^{a,-1}_{rs}\left(q^{a,*}_{rs}\right)\right) q^a_{rs} \geq 0. \tag{B.1b}$$

Combing Eq. (B.1a) and Eq. (B.1b) over the origin, destination and parking location, respectively, yields:

$$\sum_{(r,s)\in M} \sum_{p} \left(c^{a,*}_{rs,p} - c^a_{rs}\right)\left(q^a_{rs,p} - q^{a,*}_{rs,p}\right) \geq 0, \tag{B.2a}$$

$$\sum_{(r,s)\in M} \left(c^a_{rs} - f^{a,-1}_{rs}\left(q^{a,*}_{rs}\right)\right)\left(q^a_{rs} - q^{a,*}_{rs}\right) \geq 0. \tag{B.2b}$$

Summing the above two equations gives rise to:

$$
\begin{aligned}
&\left(c^a_{rs} - f^{a,-1}_{rs}\left(q^{a,*}_{rs}\right)\right) q^{a,*}_{rs} = 0; \left(c^a_{rs} - f^{a,-1}_{rs}\left(q^{a,*}_{rs}\right)\right) q^{a}_{rs} \geq 0 \\
&\Longrightarrow \sum_{(r,s)\in M} \sum_p c^{a,*}_{rs,p}(q^a_{rs,p} - q^{a,*}_{rs,p}) - \sum_{(r,s)\in M} \sum_p c^a_{rs}(q^a_{rs,p} - q^{a,*}_{rs,p}) + \sum_{(r,s)\in M} c^a_{rs}\left(q^a_{rs} - q^{a,*}_{rs}\right) - \sum_{(r,s)\in M} f^{a,-1}_{rs}\left(q^{a,*}_{rs}\right)\left(q^a_{rs} - q^{a,*}_{rs}\right) \geq 0 \\
&\Longrightarrow \sum_{(r,s)\in M} \sum_p c^{a,*}_{rs,p}(q^a_{rs,p} - q^{a,*}_{rs,p}) - \sum_{(r,s)\in M} \left(c^a_{rs} \sum_p (q^a_{rs,p} - q^{a,*}_{rs,p}) \right) + \sum_{(r,s)\in M} c^a_{rs}\left(q^a_{rs} - q^{a,*}_{rs}\right) - \sum_{(r,s)\in M} f^{a,-1}_{rs}\left(q^{a,*}_{rs}\right)\left(q^a_{rs} - q^{a,*}_{rs}\right) \geq 0 \\
&\Longrightarrow \sum_{(r,s)\in M} \sum_p c^{a,*}_{rs,p}(q^a_{rs,p} - q^{a,*}_{rs,p}) - \sum_{(r,s)\in M} c^a_{rs}(q^a_{rs} - q^{a,*}_{rs}) + \sum_{(r,s)\in M} c^a_{rs}\left(q^a_{rs} - q^{a,*}_{rs}\right) - \sum_{(r,s)\in M} f^{a,-1}_{rs}\left(q^{a,*}_{rs}\right)\left(q^a_{rs} - q^{a,*}_{rs}\right) \geq 0 \\
&\Longrightarrow \sum_{(r,s)\in M} \sum_p c^{a,*}_{rs,p}(q^a_{rs,p} - q^{a,*}_{rs,p}) - \sum_{(r,s)\in M} f^{a,-1}_{rs}\left(q^{a,*}_{rs}\right)\left(q^a_{rs} - q^{a,*}_{rs}\right) \geq 0. \qquad \text{(B.3)}
\end{aligned}
$$

This indicates that the first two terms in the VI formulation should be no less than zero based on the equilibrium conditions with respect to the PAV demand and parking choice.

We now look at the third and the fifth terms regarding route choices of PAVs and OD-SAVs in the VI formulation in Eq. (14). Similarly, given the PAV demand and parking choice, it is well-known that the route choice equilibrium conditions in Eq. (13) following the UE principle (Yang et al., 2007) can be reformulated as follows:

$$\sum_{e\in E} t_e\left(x^*_e\right)\left(x^a_e - x^{a,*}_e\right) \geq 0, \qquad \text{(B.4a)}$$

$$\sum_{e\in E} t_e\left(x^*_e\right)\left(x^b_e - x^{b,*}_e\right) \geq 0. \qquad \text{(B.4b)}$$

For the OD-SAV demand equilibrium represented by the fourth term in Eq. (14), given the link flow pattern, based on the equilibrium conditions in Eq. (11), one can readily identify:

$$
\begin{aligned}
&\left(\overline{c}^b_{rs} - f^{b,-1}_{rs}\left(q^{b,*}_{rs}\right)\right) q^{b,*}_{rs} = 0; \left(\overline{c}^b_{rs} - f^{b,-1}_{rs}\left(q^{b,*}_{rs}\right)\right) q^{b}_{rs} \geq 0 \\
&\Longrightarrow \sum_{(r,s)\in M} \left(\overline{c}^b_{rs} - f^{b,-1}_{rs}\left(q^{b,*}_{rs}\right)\right)\left(q^b_{rs} - q^{b,*}_{rs}\right) \geq 0 \\
&\Longrightarrow \sum_{(r,s)\in M} \overline{c}^b_{rs}\left(q^b_{rs} - q^{b,*}_{rs}\right) - \sum_{(r,s)\in M} f^{b,-1}_{rs}\left(q^{b,*}_{rs}\right)\left(q^b_{rs} - q^{b,*}_{rs}\right) \geq 0. \qquad \text{(B.5)}
\end{aligned}
$$

Given the link flow pattern, one can further verify that $\sum_{(r,s)\in M} \overline{c}^b_{rs}\left(q^b_{rs} - q^{b,*}_{rs}\right) = 0$ based on the OD-SAV demand function in Eq. (4), and we have:

$$-\sum_{(r,s)\in M} f^{b,-1}_{rs}\left(q^{b,*}_{rs}\right)\left(q^b_{rs} - q^{b,*}_{rs}\right) \geq 0. \qquad \text{(B.6)}$$

Combining the above results, one can derive the VI formulation in Eq. (14) (as a result of the equilibrium conditions defined in Eqs. (10)-(13)).

Sufficiency: VI $\Longrightarrow$ Joint user equilibrium

Eq. (14) holds for any feasible PAV demand $\boldsymbol{q^a} = \{q^a_{rs}\}$, OD-SAV demand $\boldsymbol{q^b} = \left\{q^b_{rs}\right\}$, parking choice $\boldsymbol{q_p} = \left\{q^a_{rs,p}\right\}$ and link flow pattern $\boldsymbol{x^a} = \{x^a_e\}$, $\boldsymbol{x^b} = \left\{x^b_e\right\}$. Let $x^a_e = x^{a,*}_e$ and $x^b_e = x^{b,*}_e$ for each link $e \in E$, according to the OD-SAV demand function in Eq. (5a), one can readily identify that $\sum_{(r,s)\in M} f^{b,-1}_{rs}\left(q^{b,*}_{rs}\right)\left(q^b_{rs} - q^{b,*}_{rs}\right) = 0$. Then, the following results can be obtained based on the VI formulation in Eq. (14):

$$\sum_{(r,s)\in M} \sum_p c^{a,*}_{rs,p}(q^a_{rs,p} - q^{a,*}_{rs,p}) - \sum_{(r,s)\in M} f^{a,-1}_{rs}\left(q^{a,*}_{rs}\right)\left(q^a_{rs} - q^{a,*}_{rs}\right) \geq 0, \qquad \text{(B.7a)}$$

$$\Longrightarrow \sum_{(r,s)\in M} \sum_p c^{a,*}_{rs,p} q^a_{rs,p} - \sum_{(r,s)\in M} f^{a,-1}_{rs}\left(q^{a,*}_{rs}\right) q^a_{rs} \geq \sum_{(r,s)\in M} \sum_p c^{a,*}_{rs,p} q^{a,*}_{rs,p} - \sum_{(r,s)\in M} f^{a,-1}_{rs}\left(q^{a,*}_{rs}\right) q^{a,*}_{rs}. \qquad \text{(B.7b)}$$

This means that $(q_{rs}^{a,*}, q_{rs,p}^{a,*})$ is the solution to the following optimization problem:

$$\underset{q_{rs}^a \geq 0, q_{rs,p}^a \geq 0}{Min} \quad \sum_{(r,s)\in M} \sum_{p} c_{rs,p}^{a,*} q_{rs,p}^{a} - \sum_{(r,s)\in M} f_{rs}^{a,-1}\left(q_{rs}^{a,*}\right) q_{rs}^{a}, \tag{B.8}$$

subject to $\sum_p q_{rs,p}^a = q_{rs}^a$ for any OD pair (r, s). One can readily verify that the Karush-Kuhn-Tucker (KKT) conditions of the minimization optimization problem are identical to the parking choice equilibrium conditions in Eq. (12), which exactly corresponds to the parking choice equilibrium.

Furthermore, given the equilibrium PAV demand $\boldsymbol{q^{a,*}}$ and parking choice $\boldsymbol{q_p^*}$, based on the VI formulation in Eq. (14), we can obtain the following:

$$\begin{aligned} &\sum_{e\in E} t_e\left(x_e^*\right)\left(x_e^a - x_e^{a,*}\right) + \sum_{e\in E} t_e\left(x_e^*\right)\left(x_e^b - x_e^{b,*}\right) \Longleftrightarrow \sum_{e\in E} t_e\left(x_e^*\right)\left(x_e - x_e^*\right) \geq 0 \\ &\Longleftrightarrow \sum_{r'} \sum_{s'} \sum_{W_{rs}} t_{rs,w}^{*}(f_{rs,w} - f_{rs,w}^{*}) \geq 0. \end{aligned} \tag{B.9}$$

This means that $f_{rs,w}^*$ is the solution to the following minimization problem:

$$\underset{f_{rs,w}^* \geq 0}{Min} \quad \sum_{(r,s)\in M} \sum_{W_{rs}} t_{rs,w}^{*} f_{rs,w}, \tag{B.10}$$

subject to $\sum_{W_{rs}} f_{rs,w} = Q_{rs}^{a,*} + y_{rs}$. Similarly, the VI in Eq. (B.9) is equivalent to Eq. (B.10), since the Karush-Kuhn-Tucker (KKT) conditions are identical.

The above proofs of the necessity and sufficiency demonstrate that the VI problem in Eq. (14) is equivalent to the equilibrium conditions in Eqs. (10)-(13). This completes the proof. □

Appendix C. Proof of Proposition 3.3

Proof. Given the PAV demand $\boldsymbol{q^{a,*}} = \{q_{rs}^{a,*}\}$, suppose we have two different parking choice solutions $\boldsymbol{q_p'} = \left\{q_{rs,p}^{a,'}\right\}$ and $\boldsymbol{q_p''} = \left\{q_{rs,p}^{a,''}\right\}$, where $q_{rs,p}^{a,'} \neq q_{rs,p}^{a,''}$ for at least one parking location $p \in P$ of travelers between one OD pair (r, s). Based on Proposition 3.2, given PAV demand $\boldsymbol{q^{a,*}}$ and parking choice $\boldsymbol{q_p}$, the OD-SAV demand $\boldsymbol{q^b}$ and the link flow pattern $\boldsymbol{x}$ can be uniquely determined. Thus, we can obtain the unique OD-SAV demand denoted by $\boldsymbol{q^{b,'}}$ and $\boldsymbol{q^{b,''}}$ and link flow pattern denoted by $\boldsymbol{x'}$ and $\boldsymbol{x''}$ under the two different parking choice solutions $\boldsymbol{q_p'}$ and $\boldsymbol{q_p''}$. Given the same equilibrium PAV demand $\boldsymbol{q^{a,*}}$, substituting the two solutions $(\boldsymbol{q_p'}, \boldsymbol{q^{b,'}}, \boldsymbol{x'})$ and $(\boldsymbol{q_p''}, \boldsymbol{q^{b,''}}, \boldsymbol{x''})$ into Eq. (14) we have:

$$\sum_{(r,s)\in M} \sum_{p} c_{rs,p}^{a,'}(q_{rs,p}^{a,''} - q_{rs,p}^{a,'}) - \sum_{(r,s)\in M} f_{rs}^{b,-1}\left(q_{rs}^{b,'}\right)\left(q_{rs}^{b,''} - q_{rs}^{b,'}\right) + \sum_{e} t_e(x_e')(x_e'' - x_e') \geq 0, \tag{C.1a}$$

$$\sum_{(r,s)\in M} \sum_{p} c_{rs,p}^{a,''}(q_{rs,p}^{a,'} - q_{rs,p}^{a,''}) - \sum_{(r,s)\in M} f_{rs}^{b,-1}\left(q_{rs}^{b,''}\right)\left(q_{rs}^{b,'} - q_{rs}^{b,''}\right) + \sum_{e} t_e(x_e'')(x_e' - x_e'') \geq 0. \tag{C.1b}$$

Combining the two equations in Eq. (C.1), we can derive:

$$\begin{aligned} &\sum_{(r,s)\in M} \sum_{p} \left(c_{rs,p}^{a,'} - c_{rs,p}^{a,''}\right)(q_{rs,p}^{a,''} - q_{rs,p}^{a,'}) - \sum_{(r,s)\in M} \left(f_{rs}^{b,-1}\left(q_{rs}^{b,'}\right) - f_{rs}^{b,-1}\left(q_{rs}^{b,''}\right)\right)\left(q_{rs}^{b,''} - q_{rs}^{b,'}\right) \\ &+ \sum_{e} \left(t_e(x_e') - t_e(x_e'')\right)\left(x_e'' - x_e'\right) \geq 0. \end{aligned} \tag{C.2}$$

With the parking choice equilibrium conditions defined in Eq. (12), we always have $c_{rs,p}^{a,'} = c_{rs,p}^{a,''} = c_{rs}^{a}$, and thus the first term in Eq. (C.2) can be eliminated. We then have:

$$\sum_{e} \left(t_e(x_e') - t_e(x_e'')\right)\left(x_e'' - x_e'\right) - \sum_{(r,s)\in M} \left(f_{rs}^{b,-1}\left(q_{rs}^{b,'}\right) - f_{rs}^{b,-1}\left(q_{rs}^{b,''}\right)\right)\left(q_{rs}^{b,''} - q_{rs}^{b,'}\right) \geq 0. \tag{C.3}$$

Furthermore, under the assumption that the travel time function is strictly increasing with the link flow and the demand function is strictly decreasing with the travel cost, we have:

$$\left(t_e(x_e') - t_e(x_e'')\right)\left(x_e'' - x_e'\right) \le 0, \forall e \in E \implies \sum_e \left(t_e(x_e') - t_e(x_e'')\right)\left(x_e'' - x_e'\right) \le 0, \tag{C.4a}$$

$$\begin{aligned} &-\left(f_{rs}^{b,-1}\left(q_{rs}^{b,'}\right) - f_{rs}^{b,-1}\left(q_{rs}^{b,''}\right)\right)\left(q_{rs}^{b,''} - q_{rs}^{b,'}\right) \le 0, \forall r \in R, s \in S \\ &\implies -\sum_{(r,s)\in M}\left(f_{rs}^{b,-1}\left(q_{rs}^{b,'}\right) - f_{rs}^{b,-1}\left(q_{rs}^{b,''}\right)\right)\left(q_{rs}^{b,''} - q_{rs}^{b,'}\right) \le 0. \end{aligned} \tag{C.4b}$$

Clearly, only when $\boldsymbol{x'} = \boldsymbol{x''}$ and $\boldsymbol{q^{b,'}} = \boldsymbol{q^{b,''}}$, Eq. (C.3) holds, otherwise it contradicts Eq. (C.4). Therefore, $(\boldsymbol{x'}, \boldsymbol{q^{b,'}})$ and $(\boldsymbol{x''}, \boldsymbol{q^{b,''}})$ must be identical. This completes the proof. □

Appendix D. Proof of Proposition 3.4

Proof. Suppose that at the equilibrium the PAV demand pattern is not unique, then there must exist two different PAV demand solutions denoted as $\boldsymbol{q^{a,'}} = \left\{q_{rs}^{a,'}\right\}$ and $\boldsymbol{q^{a,''}} = \left\{q_{rs}^{a,''}\right\}$, where $q_{rs}^{a,'} \neq q_{rs}^{a,''}$ for at least one OD pair. Based on Proposition 3.3, given PAV demand pattern $\boldsymbol{q^{a,'}}$ and $\boldsymbol{q^{a,''}}$, and parking choice $\boldsymbol{q_p'}$ and $\boldsymbol{q_p''}$, the unique flow pattern and OD-SAV demand $\left(\boldsymbol{x'}, \boldsymbol{q^{b,'}}\right)$ and $\left(\boldsymbol{x''}, \boldsymbol{q^{b,''}}\right)$ can be determined, respectively. Clearly, the VI formulation defined in Eq. (14) holds for any feasible $(\boldsymbol{q^a}, \boldsymbol{q^b}, \boldsymbol{q_p}, \boldsymbol{x})$. If we let $\boldsymbol{q_p} = \boldsymbol{q_p^*}$, based on Eq. (14), we can obtain:

$$\sum_{e\in E} t_e\left(x_e^*\right)\left(x_e - x_e^*\right) - \sum_{(r,s)\in M} f_{rs}^{a,-1}\left(q_{rs}^{a,*}\right)\left(q_{rs}^{a} - q_{rs}^{a,*}\right) - \sum_{(r,s)\in M} f_{rs}^{b,-1}\left(q_{rs}^{b,*}\right)\left(q_{rs}^{b} - q_{rs}^{b,*}\right) \ge 0. \tag{D.1}$$

Substituting the two equilibrium solutions $(\boldsymbol{q^{a,'}}, \boldsymbol{q^{b,'}}, \boldsymbol{x'})$ and $(\boldsymbol{q^{a,''}}, \boldsymbol{q^{b,''}}, \boldsymbol{x''})$ into Eq. (D.1), we can derive:

$$\sum_e t_e(x_e')(x_e'' - x_e') - \sum_{(r,s)\in M} f_{rs}^{a,-1}\left(q_{rs}^{a,'}\right)\left(q_{rs}^{a,''} - q_{rs}^{a,'}\right) - \sum_{(r,s)\in M} f_{rs}^{b,-1}\left(q_{rs}^{b,'}\right)\left(q_{rs}^{b,''} - q_{rs}^{b,'}\right) \ge 0, \tag{D.2a}$$

$$\sum_e t_e(x_e'')(x_e' - x_e'') - \sum_{(r,s)\in M} f_{rs}^{a,-1}\left(q_{rs}^{a,''}\right)\left(q_{rs}^{a,'} - q_{rs}^{a,''}\right) - \sum_{(r,s)\in M} f_{rs}^{b,-1}\left(q_{rs}^{b,''}\right)\left(q_{rs}^{b,'} - q_{rs}^{b,''}\right) \ge 0. \tag{D.2b}$$

Combining Eq. (D.2a) and Eq. (D.2b), we can further obtain:

$$\begin{aligned} &\sum_e \left(t_e(x_e') - t_e(x_e'')\right)\left(x_e'' - x_e'\right) - \sum_{(r,s)\in M}\left(f_{rs}^{a,-1}\left(q_{rs}^{a,'}\right) - f_{rs}^{a,-1}\left(q_{rs}^{a,''}\right)\right)\left(q_{rs}^{a,''} - q_{rs}^{a,'}\right) \\ &- \sum_{(r,s)\in M}\left(f_{rs}^{b,-1}\left(q_{rs}^{b,'}\right) - f_{rs}^{b,-1}\left(q_{rs}^{b,''}\right)\right)\left(q_{rs}^{b,''} - q_{rs}^{b,'}\right) \ge 0. \end{aligned} \tag{D.3}$$

Under the assumption that the travel time function is strictly increasing with the link flow and the demand function is strictly decreasing with the travel cost, we have:

$$\left(t_e(x_e') - t_e(x_e'')\right)\left(x_e'' - x_e'\right) \le 0, \forall e \in E \implies \sum_e \left(t_e(x_e') - t_e(x_e'')\right)\left(x_e'' - x_e'\right) \le 0, \tag{D.4a}$$

$$\begin{aligned} &-\left(f_{rs}^{a,-1}\left(q_{rs}^{a,'}\right) - f_{rs}^{a,-1}\left(q_{rs}^{a,''}\right)\right)\left(q_{rs}^{a,''} - q_{rs}^{a,'}\right) \le 0, \forall r \in R, s \in S \\ &\implies -\sum_{(r,s)\in M}\left(f_{rs}^{a,-1}\left(q_{rs}^{a,'}\right) - f_{rs}^{a,-1}\left(q_{rs}^{a,''}\right)\right)\left(q_{rs}^{a,''} - q_{rs}^{a,'}\right) \le 0, \end{aligned} \tag{D.4b}$$

$$\begin{aligned} &-\left(f_{rs}^{b,-1}\left(q_{rs}^{b,'}\right) - f_{rs}^{b,-1}\left(q_{rs}^{b,''}\right)\right)\left(q_{rs}^{b,''} - q_{rs}^{b,'}\right) \le 0, \forall r \in R, s \in S \\ &\implies -\sum_{(r,s)\in M}\left(f_{rs}^{b,-1}\left(q_{rs}^{b,'}\right) - f_{rs}^{b,-1}\left(q_{rs}^{b,''}\right)\right)\left(q_{rs}^{b,''} - q_{rs}^{b,'}\right) \le 0. \end{aligned} \tag{D.4c}$$

Clearly, only when $\boldsymbol{x'} = \boldsymbol{x''}$, $\boldsymbol{q^{b,'}} = \boldsymbol{q^{b,''}}$ and $\boldsymbol{q^{a,'}} = \boldsymbol{q^{a,''}}$, Eq. (D.3) holds, otherwise it contradicts Eq. (D.4). Therefore, $(\boldsymbol{x'}, \boldsymbol{q^{a,'}}, \boldsymbol{q^{b,'}})$ and $(\boldsymbol{x''}, \boldsymbol{q^{a,''}}, \boldsymbol{q^{b,''}})$ must be identical. This completes the proof. □

Appendix E. Link flow pattern and the OD specific trip fare

Table E.6 The link information and equilibrium flow solutions

Link a	Length (km)	Free travel time $t_{e,0}$ (min)	Coefficient ($\xi_e/10^{-3}$)	P-JUE	SW-JUE	P-JME	SW-JME
1-2	16.0	8.73	1.01	3314	3744	1165	1363
1-8	9.0	6.75	1.01	3621	3619	1434	246
2-1	16.0	8.73	1.01	880	1159	378	462
2-7	3.5	2.63	0.39	7118	6191	1526	1099
2-12	5.6	4.20	0.63	7666	7805	2230	3086
3-6	7.2	5.40	0.81	1519	2689	1127	1677
3-9	24.4	14.64	1.83	952	2531	1069	2340
4-5	3.5	2.63	0.39	2132	2676	794	2033
4-13	4.3	3.19	0.48	3921	4433	1354	2083
5-4	3.5	2.63	0.39	4735	5624	2383	2271
5-6	8.0	4.80	0.60	10030	9516	1582	2021
5-10	7.8	5.85	0.88	5008	5094	1746	2223
6-3	7.2	5.40	0.81	9929	9944	1823	2021
6-5	8.0	4.80	0.60	2204	2744	1131	1679
7-2	3.5	2.63	0.39	1840	1047	263	510
7-8	12.2	9.15	1.37	6448	4268	1438	1187
7-9	9.5	5.70	0.71	1567	2228	694	1083
8-1	9.0	6.75	1.01	2951	3266	1392	1121
8-7	12.2	9.15	1.37	740	992	257	506
8-9	12.0	9.00	1.35	2609	2960	1258	1140
9-3	24.4	14.64	1.83	2113	3611	1665	2141
9-7	9.5	5.70	0.71	1113	906	775	1008
9-8	12.0	9.00	1.35	4703	5363	1679	1553
10-5	7.8	5.85	0.88	9136	8775	2102	2475
10-12	5.5	4.13	0.62	7503	7058	1982	2241
10-13	2.5	1.88	0.28	10780	9764	2246	1903
10-14	5.3	3.98	0.60	6669	7626	2300	2083
10-18	7.6	5.70	0.86	4857	5481	1943	1967
11-13	4.8	3.60	0.54	1098	2811	1442	2076
11-16	4.0	3.00	0.45	9941	10233	2390	2536
12-2	5.6	4.20	0.63	8156	7961	2240	2761
12-10	5.5	4.13	0.62	5914	5257	1555	1983
12-14	5.7	4.28	0.64	6384	6247	2181	2001
13-4	4.3	3.19	0.48	9333	9554	2649	2586
13-10	2.5	1.88	0.28	6506	6793	1856	1724
14-10	5.3	3.98	0.60	5831	6246	1878	2217
14-12	5.7	4.28	0.64	628	60	705	1234
14-15	2.3	1.38	0.17	6484	7234	1398	2820
13-11	4.8	3.60	0.54	3954	4440	1377	2041
15-14	2.3	1.38	0.17	7871	7646	2947	3015
15-18	4.3	3.23	0.48	4970	5439	1321	1872
16-11	4.0	3.00	0.45	1093	2803	865	1916
16-18	4.0	3.00	0.45	6243	6812	1985	2167
17-18	3.9	2.93	0.44	9389	9581	1621	2653
18-10	7.6	5.70	0.86	9342	8955	2164	2368
18-15	4.3	3.23	0.48	714	401	1270	1458
18-16	4.0	3.00	0.45	4882	6924	2059	2274
18-17	3.9	2.93	0.44	15024	15538	2607	3018

Table E.7 The trip fare for OD-SAV service of all OD pairs

OD pair	P-JUE	SW-JUE	P-JME	SW-JME
1	8.36	0.14	8.37	0.13
2	8.36	0.16	8.39	0.17
3	8.37	0.17	8.41	0.18
4	8.23	0.13	8.26	0.12
5	8.12	0.14	8.16	0.13
6	8.82	0.13	8.86	0.15
7	8.67	0.17	8.66	0.14
8	8.53	0.16	8.53	0.14
9	8.56	0.17	8.59	0.19
10	8.54	0.14	8.58	0.15
11	8.42	0.17	8.47	0.15
12	8.53	0.16	8.54	0.14
13	8.41	0.17	8.42	0.16
14	8.44	0.15	8.43	0.12
15	8.4	0.17	8.43	0.17
16	8.59	0.17	8.6	0.19
17	8.51	0.15	8.54	0.16
18	8.27	0.16	8.33	0.18
19	8.1	0.13	8.16	0.16
20	8.7	0.14	8.68	0.16
21	8.12	0.15	8.15	0.14
22	8.5	0.17	8.51	0.14
23	8.05	0.12	8.09	0.16
24	8.04	0.14	8.08	0.12
25	8.21	0.16	8.24	0.18
26	8.86	0.16	8.89	0.18
27	8.7	0.14	8.73	0.16
28	8.23	0.13	8.29	0.14
29	8.42	0.15	8.44	0.15

Appendix F. Lower-level solution variation with iterations of upper-level problem

In this Appendix, we present the lower-level solution convergence and variation of solutions with the iterated upper-level solution. Specifically, for each iteration of upper-level decision, we compute the equilibrium link flows when the lower-level traffic assignment problem reaches the convergence criteria set up in Algorithm 1 or 2, and calculate the percentage change of link flows compared with the last iteration of upper-level decision. The minimum, maximum, median, and quartile values of the link flow percentage changes are presented in the box plot in Fig. F.8. As shown, with the evolvement of upper-level decision, the median of link flow percentage change moves towards zero. The variation of link flow percentage change also diminishes as the length of box reduces. This indicates that the evolution of upper-level decision tends to lessen the variation of lower-level link flow solutions.

Moreover, the number of iterations needed for the lower-level problem to converge at each iteration of upper-level decision is presented in Fig. F.9. The results suggest that, as upper-level decision evolves, the required numbers of iterations exhibit decreasing trend in profit-maximization scenarios in Fig. F.9a, while those in social welfare-maximization scenarios generally increase in Fig. F.9b. It takes more iterations for the lower-level problem to converge in social welfare-maximization scenarios.

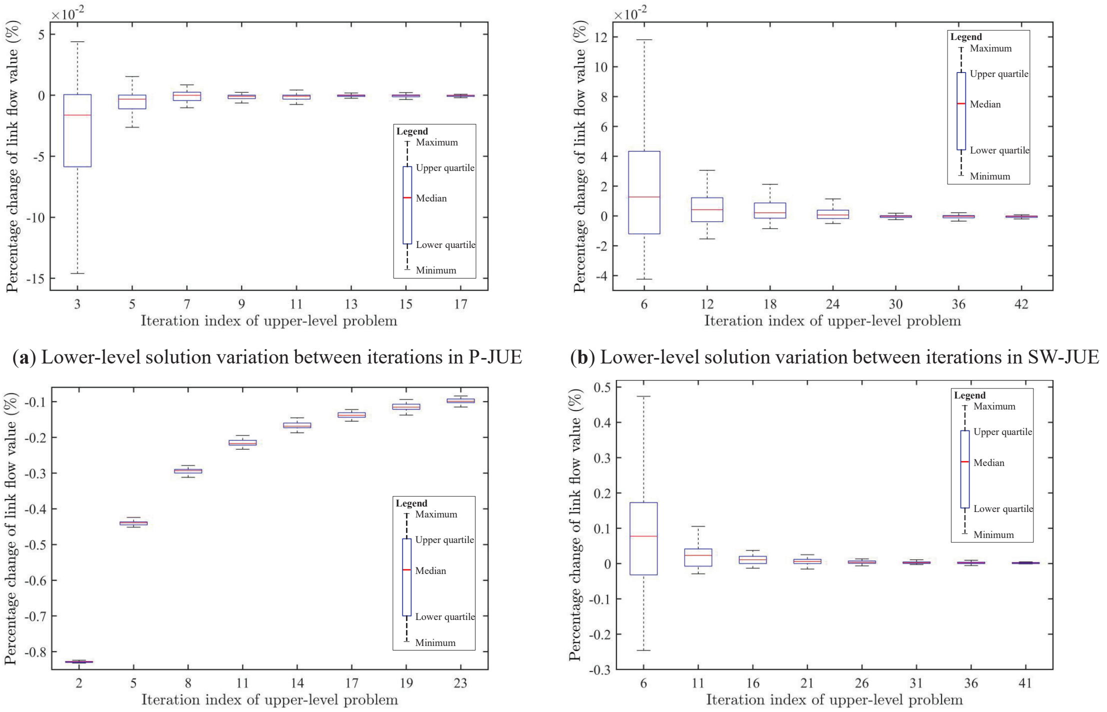

(**a**) Lower-level solution variation between iterations in P-JUE (**b**) Lower-level solution variation between iterations in SW-JUE

(**c**) Lower-level solution variation between iterations in P-JME (**d**) Lower-level solution variation between iterations in SW-JME

Fig. F.8. Percentage change of lower-level solution across iterations of upper-level problem

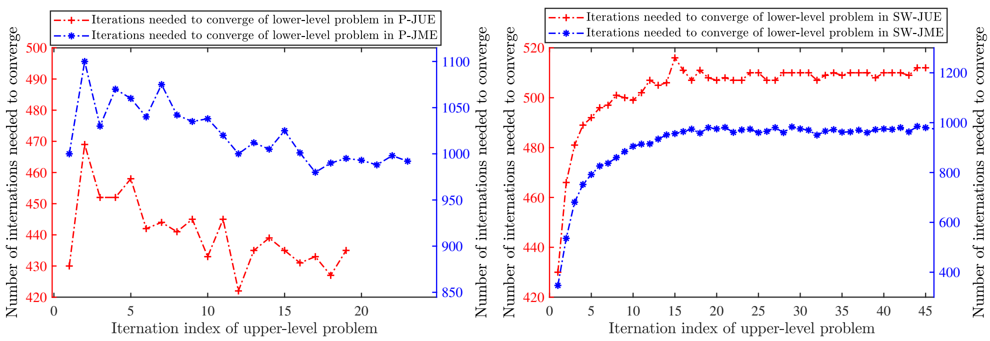

(**a**) The profit-maximization scenario (**b**) The social welfare-maximization scenario

Fig. F.9. The required number of iterations for lower-level solution convergence at each iteration of upper-level problem

References

Ainsalu, J., Arffman, V., Bellone, M., Ellner, M., Haapamäki, T., Haavisto, N., Josefson, E., Ismailogullari, A., Lee, B., Madland, O. et al. (2018). State of the art of automated buses. *Sustainability*, *10*, 3118.

Bahk, Y., Hyland, M. F., & An, S. (2022). Private autonomous vehicles and their impacts on near-activity location travel patterns: Integrated mode choice and parking assignment model. *Transportation Research Record*, *2676*, 276–295.

Burns, L. D. (2013). A vision of our transport future. *Nature*, *497*, 181–182.

Cen, X., Lo, H. K., Li, L., & Lee, E. (2018). Modeling electric vehicles adoption for urban commute trips. *Transportation Research Part B: Methodological*, *117*, 431–454.

Chen, R., & Levin, M. W. (2019). Dynamic user equilibrium of mobility-on-demand system with linear programming rebalancing strategy. *Transportation Research Record*, *2673*, 447–459.

Chen, Y., & Liu, Y. (2022). Integrated optimization of planning and operations for shared autonomous electric vehicle systems. *Transportation Science*, .

Chen, Z., He, F., Yin, Y., & Du, Y. (2017). Optimal design of autonomous vehicle zones in transportation networks. *Transportation Research Part B: Methodological*, *99*, 44–61.

Chen, Z., Spana, S., Yin, Y., & Du, Y. (2019). An advanced parking navigation system for downtown parking. *Networks and Spatial Economics*, *19*, 953–968.

Dafermos, S. (1980). Traffic equilibrium and variational inequalities. *Transportation Science*, *14*, 42–54.

Facchinei, F., & Pang, J.-S. (2007). *Finite-dimensional variational inequalities and complementarity problems*. Springer Science & Business Media.

Fagnant, D. J., & Kockelman, K. M. (2018). Dynamic ride-sharing and fleet sizing for a system of shared autonomous vehicles in austin, texas. *Transportation*, *45*, 143–158.

Golbabaei, F., Yigitcanlar, T., & Bunker, J. (2021). The role of shared autonomous vehicle systems in delivering smart urban mobility: A systematic review of the literature. *International Journal of Sustainable Transportation*, *15*, 731–748.

Graham, D. J., & Glaister, S. (2004). Road traffic demand elasticity estimates: a review. *Transport reviews*, *24*, 261–274.

Gu, Z., Najmi, A., Saberi, M., Liu, W., & Rashidi, T. H. (2020). Macroscopic parking dynamics modeling and optimal real-time pricing considering cruising-for-parking. *Transportation Research Part C: Emerging Technologies*, *118*, 102714.

Guo, H., Chen, Y., & Liu, Y. (2022). Shared autonomous vehicle management considering competition with human-driven private vehicles. *Transportation research part C: emerging technologies*, *136*, 103547.

Gurumurthy, K. M., & Kockelman, K. M. (2018). Analyzing the dynamic ride-sharing potential for shared autonomous vehicle fleets using cellphone data from orlando, florida. *Computers, Environment and Urban Systems*, *71*, 177–185.

Han, L., Sun, H., Wang, D. Z., & Zhu, C. (2018). A stochastic process traffic assignment model considering stochastic traffic demand. *Transportmetrica B: transport dynamics*, *6*, 169–189.

Harker, P. T. (1988). Multiple equilibrium behaviors on networks. *Transportation Science*, *22*, 39–46.

He, F., Wu, D., Yin, Y., & Guan, Y. (2013). Optimal deployment of public charging stations for plug-in hybrid electric vehicles. *Transportation Research Part B: Methodological*, *47*, 87–101.

He, F., Yin, Y., & Lawphongpanich, S. (2014). Network equilibrium models with battery electric vehicles. *Transportation Research Part B: Methodological*, *67*, 306–319.

He, F., Yin, Y., & Zhou, J. (2015). Deploying public charging stations for electric vehicles on urban road networks. *Transportation Research Part C: Emerging Technologies*, *60*, 227–240.

Jian, S., Liu, W., Wang, X., Yang, H., & Waller, S. T. (2020). On integrating carsharing and parking sharing services. *Transportation Research Part B: Methodological*, *142*, 19–44.

Kang, D., Hu, F., & Levin, M. (2022). Impact of automated vehicles on traffic assignment, mode split, and parking behavior. *Transportation research part D: transport and environment*, *104*, 103200.

Ke, J., Yang, H., & Zheng, Z. (2020). On ride-pooling and traffic congestion. *Transportation Research Part B: Methodological*, *142*, 213–231.

Kinderlehrer, D., & Stampacchia, G. (2000). *An introduction to variational inequalities and their applications*. SIAM.

Levin, M. W., & Boyles, S. D. (2020). Optimal guidance algorithms for parking search with reservations. *Networks and Spatial Economics*, *20*, 19–45.

Levin, M. W., Wong, E., Nault-Maurer, B., & Khani, A. (2020). Parking infrastructure design for repositioning autonomous vehicles. *Transportation Research Part C: Emerging Technologies*, *120*, 102838.

Litman, T. (2017). *Understanding transport demands and elasticities*. Victoria Transport Policy Institute Victoria, BC, Canada.

Liu, H., & Wang, D. Z. (2015). Global optimization method for network design problem with stochastic user equilibrium. *Transportation Research Part B: Methodological*, *72*, 20–39.

Liu, W. (2018). An equilibrium analysis of commuter parking in the era of autonomous vehicles. *Transportation Research Part C: Emerging Technologies*, *92*, 191–207.

Liu, W., & Geroliminis, N. (2016). Modeling the morning commute for urban networks with cruising-for-parking: An mfd approach. *Transportation Research Part B: Methodological*, *93*, 470–494.

Liu, W., & Geroliminis, N. (2017). Doubly dynamics for multi-modal networks with park-and-ride and adaptive pricing. *Transportation Research Part B: Methodological*, *102*, 162–179.

Liu, W., Yang, H., & Yin, Y. (2014). Expirable parking reservations for managing morning commute with parking space constraints. *Transportation Research Part C: Emerging Technologies*, *44*, 185–201.

Liu, W., Zhang, F., & Yang, H. (2021). Modeling and managing the joint equilibrium of destination and parking choices under hybrid supply of curbside and shared parking. *Transportation Research Part C: Emerging Technologies*, *130*, 103301.

Mondal, A., Juri, N. R., Bhat, C. R., & Mirzaei, A. (2022). Accounting for ride-hailing and connected and autonomous vehicle empty trips in a four-step travel demand model. *Transportation Research Record*, (p. 03611981221115072).

Narayanan, S., Chaniotakis, E., & Antoniou, C. (2020). Shared autonomous vehicle services: A comprehensive review. *Transportation Research Part C: Emerging Technologies*, *111*, 255–293.

Narayanan, S., Chaniotakis, E., & Antoniou, C. (2022). Modelling reservation-based shared autonomous vehicle services: A dynamic user equilibrium approach. *Transportation Research Part C: Emerging Technologies*, *140*, 103651.

Noruzoliaee, M., Zou, B., & Liu, Y. (2018). Roads in transition: Integrated modeling of a manufacturer-traveler-infrastructure system in a mixed autonomous/human driving environment. *Transportation Research Part C: Emerging Technologies*, *90*, 307–333.

Patriksson, M. (2015). *The traffic assignment problem: models and methods*. Courier Dover Publications.

Pinto, H. K., Hyland, M. F., Mahmassani, H. S., & Verbas, I. Ö. (2020). Joint design of multimodal transit networks and shared autonomous mobility fleets. *Transportation Research Part C: Emerging Technologies*, *113*, 2–20.

Reed, S., Campbell, A. M., & Thomas, B. W. (2022). The value of autonomous vehicles for last-mile deliveries in urban environments. *Management Science*, *68*, 280–299.

Shao, C., Yang, H., Zhang, Y., & Ke, J. (2016). A simple reservation and allocation model of shared parking lots. *Transportation Research Part C: Emerging Technologies*, *71*, 303–312.

Sheffi, Y. (1985). *Urban transportation networks* volume 6. Prentice-Hall, Englewood Cliffs, NJ.

Shen, Y., Zhang, H., & Zhao, J. (2018). Integrating shared autonomous vehicle in public transportation system: A supply-side simulation of the first-mile service in singapore. *Transportation Research Part A: Policy and Practice*, *113*, 125–136.

Smith, M. J. (1979). The existence, uniqueness and stability of traffic equilibria. *Transportation Research Part B: Methodological*, *13*, 295–304.

Stocker, A., & Shaheen, S. (2018). Shared automated mobility: early exploration and potential impacts. *Road Vehicle Automation 4*, (pp. 125–139).

Su, Q., & Wang, D. Z. (2020). On the morning commute problem with distant parking options in the era of autonomous vehicles. *Transportation Research Part C: Emerging Technologies*, *120*, 102799.

Tang, Z.-Y., Tian, L.-J., & Wang, D. Z. (2021). Multi-modal morning commute with endogenous shared autonomous vehicle penetration considering parking space constraint. *Transportation Research Part E: Logistics and Transportation Review*, *151*, 102354.

Tsouros, I., Tsirimpa, A., Pagoni, I., & Polydoropoulou, A. (2021). Maas users: Who they are and how much they are willing-to-pay. *Transportation Research Part A: Policy and Practice*, *148*, 470–480.

Van Vuren, T., Van Vliet, D., & Smith, M. J. (1990). Combined equalibrium in a network with partial route guidance. In *Traffic control methods. Proceedings of the Fifth NG Foundation Conference, Santa Barbara, California*.

Wang, D. Z., Liu, H., & Szeto, W. (2015). A novel discrete network design problem formulation and its global optimization solution algorithm. *Transportation Research Part E: Logistics and Transportation Review*, *79*, 213–230.

Wang, S., Levin, M. W., & Caverly, R. J. (2021). Optimal parking management of connected autonomous vehicles: A control-theoretic approach. *Transportation Research Part C: Emerging Technologies*, *124*, 102924.

Wang, S., & Noland, R. B. (2021). What is the elasticity of sharing a ridesourcing trip? *Transportation Research Part A: Policy and Practice*, *153*, 284–305.

Wardrop, J. G. (1952). Road paper. some theoretical aspects of road traffic research. *Proceedings of the institution of civil engineers*, *1*, 325–362.

Wei, B., Saberi, M., Zhang, F., Liu, W., & Waller, S. T. (2020). Modeling and managing ridesharing in a multi-modal network with an aggregate traffic representation: A doubly dynamical approach. *Transportation Research Part C: Emerging Technologies*, *117*, 102670.

Wu, W., Liu, W., Zhang, F., & Dixit, V. (2021). A new flexible parking reservation scheme for the morning commute under limited parking supplies. *Networks and Spatial Economics*, *21*, 513–545.

Wu, W., Zhang, F., Liu, W., & Lodewijks, G. (2020). Modelling the traffic in a mixed network with autonomous-driving expressways and non-autonomous local streets. *Transportation Research Part E: Logistics and Transportation Review*, *134*, 101855.

Xie, T., & Liu, Y. (2022). Impact of connected and autonomous vehicle technology on market penetration and route choices. *Transportation Research Part C: Emerging Technologies*, *139*, 103646.

Xu, G., Yang, H., Liu, W., & Shi, F. (2018). Itinerary choice and advance ticket booking for high-speed-railway network services. *Transportation Research Part C: Emerging Technologies*, *95*, 82–104.

Yang, H., & Huang, H.-J. (2004). The multi-class, multi-criteria traffic network equilibrium and systems optimum problem. *Transportation Research Part B: Methodological*, *38*, 1–15.

Yang, H., Liu, W., Wang, X., & Zhang, X. (2013). On the morning commute problem with bottleneck congestion and parking space constraints. *Transportation Research Part B: Methodological*, *58*, 106–118.

Yang, H., Zhang, X., & Meng, Q. (2007). Stackelberg games and multiple equilibrium behaviors on networks. *Transportation Research Part B: Methodological*, *41*, 841–861.

Zhang, F., & Liu, W. (2021). An economic analysis of integrating bike sharing service with metro systems. *Transportation Research Part D: Transport and Environment*, *99*, 103008.

Zhang, F., Liu, W., Lodewijks, G., & Travis Waller, S. (2022). The short-run and long-run equilibria for commuting with autonomous vehicles. *Transportmetrica B: transport dynamics*, *10*, 803–830.

Zhang, F., Liu, W., Wang, X., & Yang, H. (2020). Parking sharing problem with spatially distributed parking supplies. *Transportation Research Part C: Emerging Technologies*, *117*, 102676.

Zhang, F., Zheng, N., Yang, H., & Geroliminis, N. (2018a). A systematic analysis of multimodal transport systems with road space distribution and responsive bus service. *Transportation Research Part C: Emerging Technologies*, *96*, 208–230.

Zhang, X., Huang, H.-J., & Zhang, H. (2008). Integrated daily commuting patterns and optimal road tolls and parking fees in a linear city. *Transportation Research Part B: Methodological*, *42*, 38–56.

Zhang, X., Liu, W., & Waller, S. T. (2019a). A network traffic assignment model for autonomous vehicles with parking choices. *Computer-Aided Civil and Infrastructure Engineering*, *34*, 1100–1118.

Zhang, X., Liu, W., Waller, S. T., & Yin, Y. (2019b). Modelling and managing the integrated morning-evening commuting and parking patterns under the fully autonomous vehicle environment. *Transportation Research Part B: Methodological*, *128*, 380–407.

Zhang, X., Rey, D., & Waller, S. T. (2018b). Multitype recharge facility location for electric vehicles. *Computer-Aided Civil and Infrastructure Engineering*, *33*, 943–965.

Zhang, X., Robson, E., & Waller, S. T. (2021). An integrated transport and economic equilibrium model for autonomous transportation systems considering parking behavior. *Computer-Aided Civil and Infrastructure Engineering*, *36*, 902–921.

Zhang, X., Yang, H., Huang, H.-J., & Zhang, H. M. (2005). Integrated scheduling of daily work activities and morning–evening commutes with bottleneck congestion. *Transportation Research Part A: Policy and Practice*, *39*, 41–60.

Zhang, Z., & Zhang, F. (2022). Ride-pooling services with differentiated pooling sizes under endogenous congestion effect. *Transportation Research Part C: Emerging Technologies*, *144*, 103883.

Zhu, Z., Qin, X., Ke, J., Zheng, Z., & Yang, H. (2020). Analysis of multi-modal commute behavior with feeding and competing ridesplitting services. *Transportation Research Part A: Policy and Practice*, *132*, 713–727.